

Wild 2 and interstellar sample collection and Earth return

P. Tsou,¹ D. E. Brownlee,² S. A. Sandford,³ F. Hörz,⁴ and M. E. Zolensky⁴

Received 25 April 2003; revised 24 June 2003; accepted 7 August 2003; published 24 October 2003.

[1] Stardust, launched in 1999, is the first mission designed to bring samples from a known, recently deflected comet, 81P/Wild 2, on 2 January 2004 and is also the first to capture newly discovered contemporary interstellar dust streaming through our solar system. The Stardust aerogel collector accomplishes Stardust's primary science and will be returned to Earth with its captured samples on 15 January 2006 in a reentry capsule. Wild 2 samples will be captured at 6.12 km/s and represent well-preserved relics of the outer regions of our solar nebula and fundamental building blocks of our planetary system. Interstellar grains captured at velocities of less than 10 km/s are expected to survive intact and represent the main repositories of condensable elements that permeate the galaxy. These solid cometary and interstellar samples will be captured in two back-to-back sample collection trays filled with variable-density aerogel. There are 132 silica aerogel capture cells of 3 cm and 1 cm thickness for the cometary and the interstellar sides, respectively. The aerogel capture cells were wedged into the sample collection trays and wrapped on all four sides with 100- μ m-thick pure aluminum foil to facilitate aerogel cell removal. The total exposed Wild 2 surface area is 1039 cm² of aerogel and 153 cm² of aluminum foil. Results from a preliminary examination for the Wild 2 samples will be reported within 9 months of sample return and for the interstellar samples a year later. After preliminary examination the samples will be transferred to the NASA Office of the Curator and made available to the general science community. *INDEX TERMS:* 6008 Planetology: Comets and Small Bodies: Composition; 6015 Planetology: Comets and Small Bodies: Dust; 6210 Planetology: Solar System Objects: Comets; 6213 Planetology: Solar System Objects: Dust; 2129 Interplanetary Physics: Interplanetary dust; *KEYWORDS:* Wild 2, comet coma dust, interstellar dust, sample return, silica aerogel, intact capture

Citation: Tsou, P., D. E. Brownlee, S. A. Sandford, F. Hörz, and M. E. Zolensky, Wild 2 and interstellar sample collection and Earth return, *J. Geophys. Res.*, 108(E10), 8113, doi:10.1029/2003JE002109, 2003.

1. Introduction

[2] Stardust's primary science goal is to capture intact samples during a flythrough of the coma of the periodic comet 81P/Wild 2 and returning them to Earth for detailed laboratory analysis. On the way to comet Wild 2, the backside of the comet sample collector will also attempt to capture contemporary interstellar particles. The instrument responsible for sample collection is the Wild 2 and Interstellar Sample Collection and Earth Return (WISCER) instrument. An embedded portion of an overall Sample Subsystem of the Stardust spacecraft, the WISCER consists largely of the Sample Tray Assembly (STA) housing aerogel capture cells (Figure 1). Since the collected samples will be captured in WISCER and reside inside of the Sample Subsystem, their proper analysis requires a full understanding of the flight components properties.

[3] Section 1 of this paper summarizes the goals of the sample science to be carried out by WISCER. The technical bases for the WISCER design are presented in section 2. The proposed instrument objectives and instrument specifications at the beginning of the flight hardware development phase are delineated in section 3. The design of the instrument is described in section 4 and its testing and flight qualifications follow in section 5. The aerogel capture cell production, installation, and documentation are contained in section 6. Finally, section 7 provides the key aspects of the Sample Subsystem's operational plan.

[4] The Stardust scientific objectives, expected science returns, overall mission design and spacecraft description are provided by Brownlee *et al.* [2003]. A model of comet 81P/Wild 2 by Sekanina can also be found in this issue. Stardust carries other instruments that will make in situ investigations of the comet. These are can also be found in this issue and include: (1) the Cometary and Interstellar Dust Analyzer [Kissel *et al.*, 2003], (2) the Dust Flux Monitor (A. J. Tuzzolino *et al.*, Dust flux monitor instrument (DFMI) for the Stardust mission to comet Wild 2, submitted to *Journal of Geophysical Research*, 2003), and (3) the Optical Navigation Camera [Newburn *et al.*, 2003]. In addition, the upper limit of the Wild 2 mass and the time

¹Jet Propulsion Laboratory, California Institute of Technology, Pasadena, California, USA.

²Astronomy Department, University of Washington, Seattle, Washington, USA.

³NASA Ames Research Center, Moffett Field, California, USA.

⁴NASA Johnson Space Center, Houston, Texas, USA.

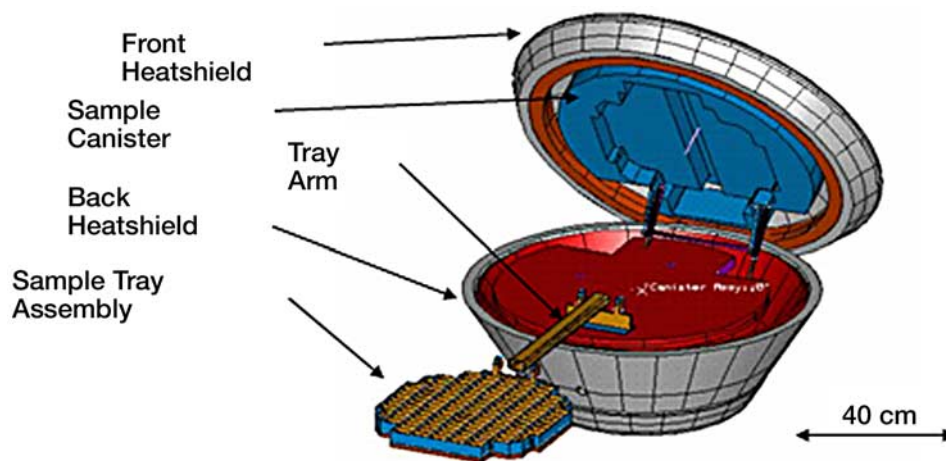


Figure 1. Stardust sample subsystem shown in the fully deployed position.

profiles of the integrated dust impacts over the cross section of the entire spacecraft can be estimated using the Doppler shifts of radio frequency signals of the spacecraft X-band transponder and large particle impact momentum may be ascertained using the Attitude Control sensors [Anderson *et al.*, 2003]. Together these in situ investigations will provide high quality data providing context for the interpretation of the captured samples.

1.1. Questions Addressed by the Wild 2 Cometary Samples

[5] The samples returned from Wild 2 are expected to be the well-preserved relics of the outer regions of the solar nebula and represent fundamental building blocks of planetary systems [Brownlee, 1989]. These samples will be the first returned from a known comet. The samples will also provide evidence for positive identification of cometary components in existing collections of meteoritic material and can contribute to understanding the following issues:

[6] 1. What is the elemental, chemical, and mineralogical composition of Wild 2 at the submicron scale? What compounds dominate the organic fraction of Wild 2?

[7] 2. To what extent are the building materials of Wild 2 found in interplanetary dust particles (IDP) and meteorites? Are IDPs consistent with Wild 2 samples? Are pyroxene-rich chondritic aggregate IDPs cometary? Are amino acids, quinones, amphiphiles, or other molecules of exobiological interest present?

[8] 3. What is the state of H₂O in Wild 2? Is it all in ice, or are there hydrated minerals?

[9] 4. Was there mixing of inner nebula materials (i.e., high-temperature condensates) in the region of comet formation in the outer nebula?

[10] 5. Are isotopic anomalies present that are signatures of the place of origin of interstellar grains? Are the high deuterium-to-hydrogen ratios seen in some IDPs common in Wild 2 solids?

[11] 6. What is the nature of the carbonaceous material in Wild 2, and what is its relationship to silicates and other mineral phases or constraining the processes by which they were formed (ion-molecule, gas-grain, irradiation of ices, etc.)? Are there organic refractory mantles on silicate

grains? Do they resemble the organics found in IDPs and meteorites?

[12] 7. Is there evidence of preaccretional processing of grains (cosmic ray tracks, sputtered rims, altered mineralogy, etc.)? Are GEMS (Glass with Embedded Fe Ni Metal and Sulfides) present?

[13] Organic compounds appear to be important components of comets [Mumma, 1997]. Organics imported to Earth by comets may have played an important role in the formation of life on the early Earth [Delsemme, 1984; Deamer *et al.*, 2002]. WISCER has no special provisions for the capture of volatile organics [Hohenberg *et al.*, 1996]; but refractory organics, such as PAHs (polycyclic aromatic hydrocarbons), captured on the surface of the collectors and embedded within solid particles will likely be retained.

1.2. Questions Addressed by the Interstellar Samples

[14] Dust grains permeate the Galaxy and are the main form of condensable elements in the interstellar medium (ISM). Dust influences nearly all types of astronomical observations and plays an important role in interstellar processes [Landgraf *et al.*, 1998]. However, most of our knowledge of interstellar dust has been necessarily indirect. The WISCER samples will be the first contemporary, free interstellar dust particles to provide direct information on the solid particles that dominate the local ISM. Analyzing interstellar dust particles from WISCER should assist in answering the following questions:

[15] 1. What is the elemental composition and compositional distribution of the interstellar grains?

[16] 2. What is the isotopic composition of H, C, N, O, Mg, Si, and other key elements? Are all the grains isotopically anomalous?

[17] 3. What is the mineralogy of the silicate grains? Are they glassy or crystalline? Do they look like GEMS?

[18] 4. What is the prevalence of grains having graphitic or related compositions? Are they abundant enough to explain the interstellar 0.22 μm extinction bump?

[19] 5. What is the extent of physical mixing of mineral phases?

[20] 6. Is there evidence of processing in the interstellar medium, such as sputtering in interstellar shocks, collisions, accretion, and chemical alteration?

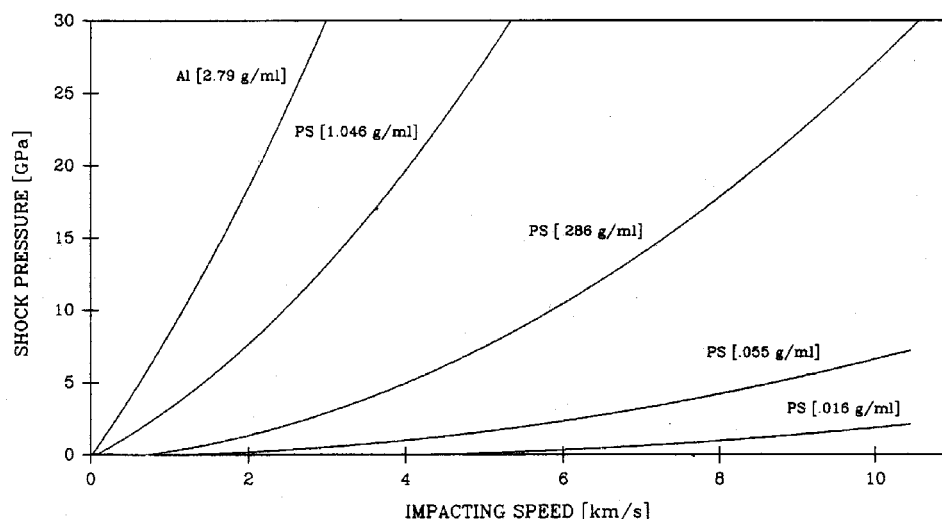


Figure 2. Shock pressure of aluminum impacting polystyrene foams of four decreasing densities.

[21] 7. Compared to the Wild 2 samples, is there evidence for differences in thermal, aqueous, or shock modifications?

2. Technology Bases

[22] Inspiration to quest for capturing cometary samples stemmed from participation with the JPL attempted missions to the last Halley apparition [Tsou, 1983]. The intact capture (retention of an unmelted portion) of hypervelocity (speeds ≥ 4 km/s) particles was originally not thought to be possible [Engelbrecht, 1986; C. L. Mader, personal communication, 1985]. However, over the past 2 decades extensive laboratory experimentation and space flight testing has demonstrated that the intact capture of hypervelocity particles at speeds up to at least 7 km/s is possible. In this section we describe the technology base enabled the WISCER including the use of ultra low-density silica aerogel as a hypervelocity particle capture medium.

2.1. Low-Density Capture Media

[23] Projectiles that impacts on metallic collector at hypervelocities are mostly atomized, allowing only for the collection of condensates [Zook and High, 1976]. Atomized capture retains the elemental compositions of the particles but destroys the sample's original morphology and mineralogical composition [Tsou, 1983]. However, guided by conversations with Charles Mader of the Los Alamos National Laboratory and experimental dynamic material properties found in the shock Hugoniot data [Marsh, 1979], Tsou noted that intact capture was possible if the capture medium has sufficiently low density [Tsou, 1990]. For example, Figure 2 shows the shock pressures experience by aluminum particles impacting polystyrene of different densities as a function of impact speed (using the graphic method of Hörz [1970]). The initial shock pressure of aluminum impacting a 16 mg/ml styrofoam at 6 km/s is about 0.8 GPa, nearly two orders of magnitude below the incipient melting point of aluminum. This raised the intriguing possibility that very low-density capture

media might be capable of achieving intact capture of hypervelocity astrophysical grains.

2.2. Early Intact Capture Experiments

[24] On the basis of this observation, an experimental development program was initiated at the NASA Ames Vertical Gun Range (AVGR) to study the hypervelocity capture properties of underdense media [Tsou *et al.*, 1984; Kromydas, 1987; Griffiths, 1989]. The laboratory experiments proceeded in four phases: large aluminum projectiles launched into underdense polymer media, large glass and geological projectiles launched into polymer media, cosmic-dust-size-range projectiles launched into polymer media, and pseudo cosmic dust composite projectiles launched into silica aerogel.

[25] The NASA AVGR is a two-stage light-gas gun capable of accelerating projectiles up to speeds of 7 km/s. The AVGR has two unique capabilities: (1) projectiles are spin released from the sabot by centripetal force; and (2) it can launch projectiles into a horizontal target at incoming angles ranging from the horizontal to the vertical. The target chamber is in full vacuum. For tests >7 km/s speeds, the electrostatic accelerator at the 2 MeV Max Planck Institut für Kernphysik at Heidelberg, the plasma drag gun at the Technische Universität of München, the two-stage light-gas gun at the Ernst Mach Institut in Freiburg Germany, and the K480 Los Alamos Hypervelocity Microparticle Impact Laboratory (a 6 Mev electrostatic accelerator) were used.

2.2.1. Large Aluminum Projectiles

[26] Since the "standard" projectile at the AVGR was aluminum, aluminum projectile capture in styrofoam dominated early experiments [Cinniger, 1986; Keyvan, 1989; Penland, 1989; Tsou and Griffiths, 1993]. The first laboratory confirmation of intact capture was achieved in April of 1983 at 5.8 km/s at the AVGR [Tsou *et al.*, 1984] with a 3.2 mm aluminum projectile captured in a 26 mg/ml commercial styrofoam. The recovered projectile retained 87% of its original mass and generated a carrot-shaped track of 54.1 cm in length.



Figure 3. Intact capture in high-density aerogel with characteristic forward fracture lines.

[27] Additional studies showed that intact capture of hypervelocity particles was not only possible but was in many respects a well-behaved process in the sense that projectile survival appeared to scale with speed and target density [Tsou, 1990]. However, it was discovered that, while low bulk density of the target medium did improve intact capture, the mesostructure of the medium plays a pivotal role in establishing the degree of intact capture within the suitable density range [Tsou *et al.*, 1991; Tsou and Albee, 1992].

2.2.2. Large Glass/Meteoritic Projectiles

[28] Successful capture of hypervelocity aluminum particles was encouraging, but tests with more reasonable cometary and interstellar analogs were clearly desirable. Glass was deemed to be a more appropriate analog for extraterrestrial silicates than aluminum. Experiments performed with soda lime and pyrex projectiles under the same condition as the large aluminum projectile experiments showed that glass projectiles followed the same capture patterns up to about 4 km/s and produced similar tracks in the capture medium [Johannessen, 1988]. At higher speeds,

these glass projectiles breakup. However, the total mass of the glass projectile was generally recovered in these experiments, but the projectile was usually found in many pieces. Additional composite projectiles were also used, including olivine, FeS, glasses, and sands held with various binders. Actual meteorites (Allende, Murchison, and Wellman) were also cored for projectiles. All these projectiles yielded similar results; that is, the projectile materials survived capture, but broke up in the polymer foam target media at speeds above 4 km/s [Tsou *et al.*, 1986].

2.2.3. Cometary Dust-Sized Projectiles

[29] After some development at the AVGR, a new cluster launch technique was invented to launch cometary particle sized projectiles at known launch speeds [Tsou *et al.*, 1988]. With this technique virtually any projectile of any size could be launched in clusters or screened for a single particle.

[30] Subsequently, a wide range of expected cometary sized projectiles were experimented with: mixtures of sieved glass beads, powdered olivine and pyrrhonite, flame sprayed olivine and FeS spheres, Hawaiian beach sands, and powdered meteoroids and lunar soils. However, it was prohibitive to sort thousands of grains to the same mass and shape. Thus, unlike the large-projectile experiments, where each projectile size, shape, integrity and mass was known precisely, the cluster projectiles were bracketed statistically. The intact capture characterization parameters (projectile recovery ratio and track length) no longer serve as useful criteria for evaluating intact capture performance, since the dispersions among the clusters are too great. Contrary to early opinion [Engelbrecht, 1986; Anderson and Ahrens, 1994], the smaller sized projectiles actually yielded higher intact recovery than larger projectiles. This phenomenon is not fully understood but may be related to increasing particle surface to volume ratio with decreasing projectile diameter.

2.2.4. Aerogel as a Capture Medium

[31] Although polymer foams proved to be successful as capturing media for hypervelocity projectiles, these materials were not compatible with deployment in space environments and it was difficult to locate and analyze particles captured in these opaque media.

[32] Intact capture of hypervelocity projectiles in silica aerogel was first successfully demonstrated using a fairly high-density aerogel [Tsou *et al.*, 1990]. However, with transparent silica aerogel it was possible to assess the condition of captured small μm sized projectile easily [Snodgrass, 1990]. These experiments showed that the projectile tracks left in high-density aerogels (150 and 88 mg/ml) resemble an inverted Christmas tree with rings



Figure 4. Intact capture in medium-density aerogel with the typical carrot track and with the particle lodged at the end of the track.



Figure 5. Intact capture in low-density aerogel shows typical long track with the particle arrested at the end of a curved hook.

of conchoidal fractures (Figure 3). However, lower density aerogels (50–20 mg/ml) produced much longer, smoother carrot-shaped tracks similar to those seen in polymer foams (Figure 4). For aerogels having densities about 10 mg/ml or less, intact projectiles were lodged about 60° from the track at the end of hooks (Figure 5). It was also found that an aerogel coating builds up around the particle during impact (Figure 6). This coating may protect the particle during deceleration [Tsou, 1995]. The aerogel density threshold below which damage severity appears to be minimal was determined to be about 50 mg/ml at impact speeds of around 6 km/s.

2.3. Space Aerogel Capture Experiments

[33] Even in the best of circumstances, laboratory experiments can only imperfectly simulate space captures. Actual in situ space capture experiments are required to fully assess the efficacy of the intact capture of actual extraterrestrial particles. The first successful space flight of an aerogel collector, the Sample Return Experiment (SRE), took place in January of 1992 on Shuttle flight STS-42. The SRE was a “hitchhiker” experiment on a Get Away Special (GAS) and consisted of 21 silica aerogel capture cells, 10 cm × 10 cm × 1 cm, mounted on top of the standard thermal insulating end cap of a GAS payload canister. This, and additional flights, demonstrated that “fragile” aerogels were quite robust for space flights if handled properly. The first space SRE flight captured three particles visible to the unaided eye, each associated with a characteristic carrot-shaped track shaped much like those produced in laboratory experiments as shown in Figure 4. Subsequent flights showed a much wider variety of particle sizes and track shapes,

reflecting the wider variety of particle sizes, morphologies, and speeds found in Earth orbit [Tsou *et al.*, 1993].

[34] Additional aerogel collectors flown in space include an external payload (1.6 m² of aerogel) on Spacehab 2 in February 1994 [Tsou, 1995], ram versus antiram collectors on the Wake Shield Experiment on STS-69, and four Mir Sample Return Experiment (MSRE) trays mounted outside of Kavant 2 of Mir from June 1996 to April 1997 [Tsou, 1997]. These and more recent aerogel laboratory and space experiments undertaken by others [Fujiwara *et al.*, 1999; Hörz *et al.*, 1998; Burchell *et al.*, 1999], validated the previous laboratory findings and demonstrated that low-density aerogels can serve as excellent capture medium for the intact capture of extraterrestrial hypervelocity particles. This technology and experience provided the bases that enabled the design of the Stardust WISCER.

3. WISCER Specifications

[35] The design of the WISCER must simultaneously satisfy a set of specifications that meet the sample science objectives of the Stardust mission, as well as practical experimental and project limitations [Brownlee *et al.*, 2003]. These specifications encompass the relative encounter speeds at time of collection, total collector surface areas, sample collection distance from the comet nucleus, and the methods of sample collection, storage, and return.

3.1. Science and Engineering Constraints for Sampling Comet Wild 2

[36] The principal goal of the Stardust mission is to capture and return a minimum of 1000 analyzable cometary particles greater than 15 μm in diameter from Wild 2 [Brownlee *et al.*, 1994]. The cometary tray of the WISCER needs to accommodate the full range of dust morphologies expected, from solid to fluffy grains, and be capable of capturing particles in the size range from submicron up to 100 μm. Cometary grains larger than 10 μm can currently be studied by a wide variety of analytic techniques. These techniques have been developed over the years to study IDPs collected in the stratosphere and interstellar grains found embedded in meteorites. Given the modeled size

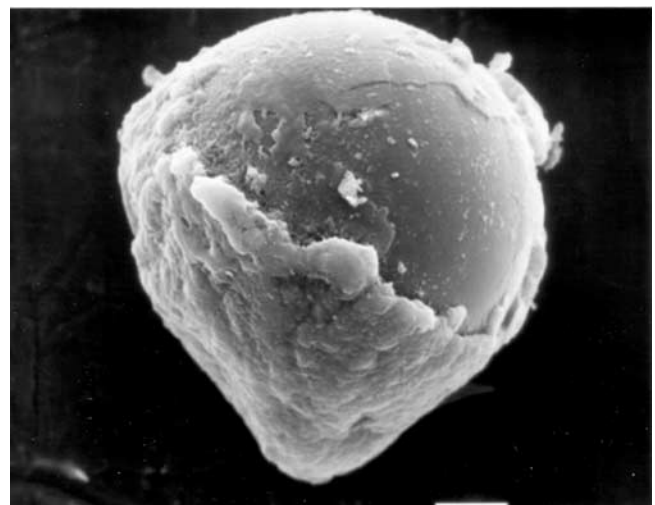


Figure 6. Coating effect in captured projectile in aerogel.

distribution of Wild 2 dust, it is expected that for every 10 μm particle, the WISCER will collect ~ 300 particles in the 1 μm size range and more than 70,000 particles in the 0.2 μm size range. Analytic techniques and equipment are continually improving and these smaller grains are expected to ultimately be amenable to study as well. Thus every effort must also be taken to control the presence of contaminants, even if very small. Within the allowed 7-year Stardust mission trajectory (C.-W. Yen, unpublished data, 1995), the available trade-space in the flyby encounter speed spanned the range from 5.4 km/s to 6.1 km/s. These velocities correspond to the time of comet encounter from 90 days preperihelion to 98.8 days postperihelion. The Stardust comet flyby has been targeted for the latest postperihelion encounter, largely based on the fact that at 98.8 days postperihelion, the heliocentric distance is 0.2 AU less, which results in an increase of available power and communication during the closest encounter period.

[37] A good degree of intact capture in aerogel has been demonstrated in laboratory experiments for speeds within the 5.4 km/s to 6.1 km/s range [Tso, 1990] and the sensitivity of intact recovery efficiency of projectiles between these speeds has been found to be small. At the expected speed of the selected intercept date, 6.12 km/s, solid grains are expected to survive mostly intact in aerogels having a density of 50 mg/ml or less. Stardust's nominal 150 km flyby encounter distance with the Wild 2 nucleus provides a reasonable balance between ensuring that sufficient sample is collected (favoring a close encounter) while minimizing the risk of catastrophic collision with a large particle (favoring a more distance encounter) and allowing for various in situ measurements (see other Stardust papers in this issue).

3.1.1. Wild 2 Observations

[38] Having had only four apparitions in its current orbit prior to the 2004 encounter, Wild 2 is not a well-known comet and had not attracted much scientific attention. Consequently, observational data on dust-to-gas mass production ratios and production rates for this comet are quite limited [Sekanina, 2003]. A working dust flux model for Wild 2 has been developed based upon light curves available from the 1978, 1984, and 1990 apparitions of Wild 2, and the Giotto dust density data from comet [McDonnell *et al.*, 1987; R. Newburn, unpublished data, 1996, 2000]. The resulting model is consistent with thermal infrared observations of the Wild 2's coma in 1997 [Hanner and Hayward, 2003].

[39] On the basis of this model, Wild 2 is expected to shed a total mass of $\sim 10^5$ tons in the form of dust during its fifth apparition. The samples swept up on the WISCER collector will represent a time compressed swath of a 0.1 m^2 cross section of the Wild 2 coma at 98.8 days after Wild 2's perihelion passage. Wild 2 is thought to be a relatively "fresh" comet, and the collected samples will likely have been processed by the solar thermal environment for only a shorter time. The closest targeted distance to the Wild 2 nucleus will nominally be 150 km, roughly the border of the parent molecule zone. At this range it is possible that unsublimed ice grains could be among the dust grains impacting on the collector. Impacting ice grains would be expected to form tracks in the aerogel, although the

Table 1. Stardust Particle Fluence/Size Distribution Model at Wild 2 150 km Encounter Distance, Postperihelion 98th Day

Particle Diameter, μm	Particles, Number/ m^{-2} > Diameter
0.2	85,700,000
0.8	21,100,000
2	4,200,000
4	559,000
8	74,400
$\rightarrow 15$	$\rightarrow 12,000$
40	751
140	81.2
1400	3.86
4000	0.25
10,000	0.0228

impacting ices will ultimately sublime and escape to space, leaving behind an empty tracks.

3.1.2. Required Aerogel Collection Area

[40] The total number of cometary particles collected during flyby is expected to vary linearly with comet nucleus miss distance (R. Newburn, unpublished data, 1996). Table 1 shows the particle size distribution expected for a 150 km encounter occurring on 2 January 2004. On the basis of laboratory simulations, it is expected that more than $\sim 90\%$ intact recovery is possible at 6 km/s for solid particles. Given that actual cometary samples may be "fluffy," a lower survival rate will be expected. If one assumes a 25% intact recovery for cometary grains, a 15 μm impacting particle would result in a 10 μm collected particle. On the basis of the modeled dust fluxes from Wild 2, a 1039 cm^2 collector area would be sufficient sweep up more than 1000 analyzable 10 μm particles, as indicated by the rightward arrow in Table 1.

[41] It should be noted that images of Wild 2 taken during previous apparitions indicate the possible presence of jets [Schulz *et al.*, 2003; Sekanina, 2003]. The dust flux within a jet can be considerably higher than the overall averaged flux, making even greater uncertainty in the dust flux at a particular location in the coma. Although the nominal encounter distance is 150 km, the final encounter distance can be adjusted to account for new information gathered prior to the encounter. Alterations of the encounter distance can only be made, however, in accordance with a preestablished Targeting Plan (Stardust, unpublished data, 1998).

3.2. Science and Engineering Constraints for Sampling Interstellar Particles

[42] The presence of contemporary, free interstellar dust in the inner heliosphere has now been confirmed by several spacecraft missions, including Ulysses and Galileo [Grün *et al.*, 1993]. This dust, which is thought to be dynamically coupled to the interstellar gas stream, enters the heliosphere at 26 km/s from the ecliptic longitude of about 252° and 2.5° latitude. Stardust will attempt to collect and return some of these particles.

3.2.1. Speed of Capture

[43] In order to capture the highest proportion of intact interstellar particles, the lowest possible capture speed is preferred. Thus it would be most advantageous to capture these particles when the spacecraft's orbit carries it in the same direction as the interstellar dust stream's velocity vector. For Stardust, this occurs as the spacecraft is on the inbound portion of its orbits. The actual capture speed of

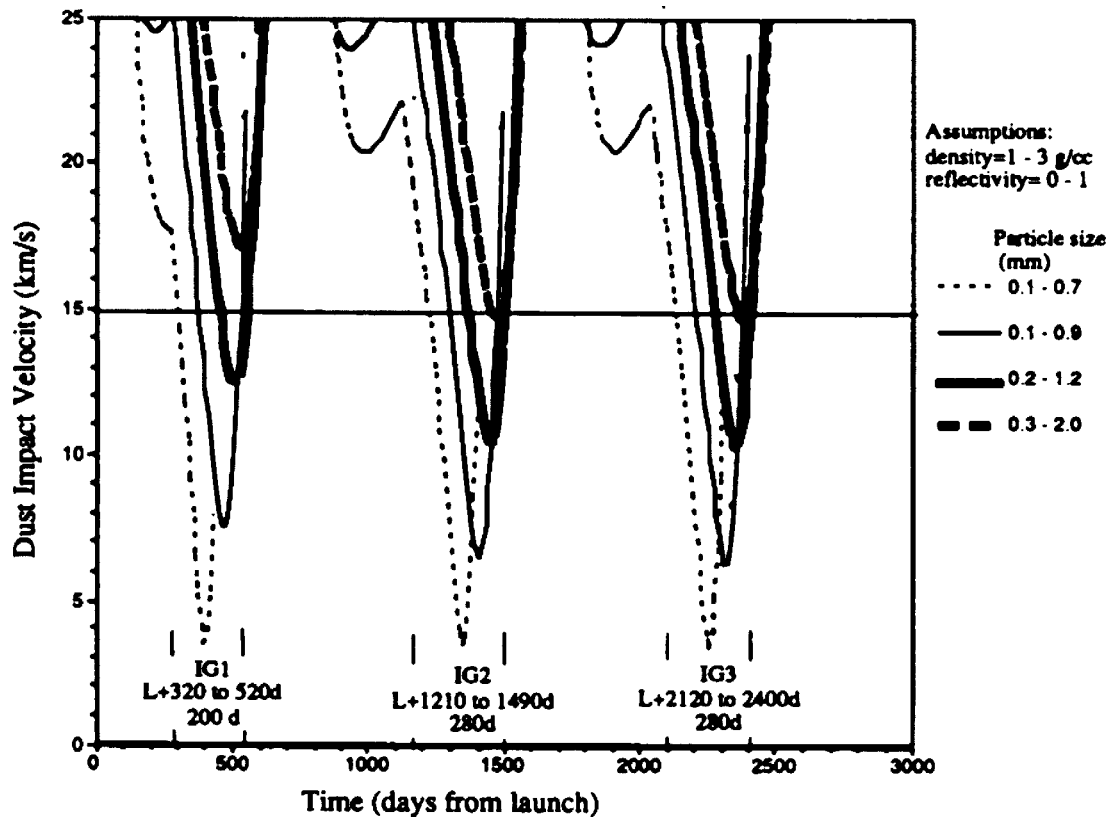


Figure 7. Speeds of interstellar particles versus sizes of particles for the three possible infall orbits.

individual interstellar particles will depend upon the balance of complex forces acting upon the particle, including solar gravity acceleration, solar radiation pressure, various other effects (e.g., Lorentz forces), and particle properties (i.e., the charge state, initial speed, size, density, and sublimation rates). To simplify the instrument specification, particles with $\beta = 1$ (the ratio of solar pressure to solar gravity) have been selected as the baseline. Figure 7 shows the modeled Stardust encounter speeds with interstellar particles for the three collection opportunities (C.-W. Yen, unpublished data, 1995), i.e., the infall portions of Stardust's three orbits of the Sun. Submicron Carbonyl iron spherules have been successfully captured in aerogel at speeds higher than 10 km/s at the dust accelerator at the Max Planck Institut. This suggests that interstellar particles may potentially be collected at encounter speeds below about 15 km/s. For particles with $\beta = 1$ (0.1–0.9 μm), significant collection time is possible for encounter speeds ranging from 7 km/s to 15 km/s during the infall portions of Stardust's three orbits.

[44] Since interstellar dust particles have a higher average speed than cometary particles, the overall density of the aerogel capture cells should have a lower average value and even lower entry density than the aerogel in the cometary capture cells. A base capture cell density of 20 mg/ml has been chosen for the interstellar aerogel capture cells.

[45] On the average, interstellar are expected to be considerably smaller than cometary particles, mostly in the submicron size range, although interstellar particles as large as 10 μm are distinctly possibility [Landgraf and

Grün, 1998]. Thus the interstellar collector was specified to accommodate the capture of solid grains of up to 10 μm .

3.2.2. Collector Area

[46] The collection of contemporary interstellar dust is secondary to the collection of the comet Wild 2 sample. As a result, the interstellar collections must accommodate any restrictions imposed by the cometary collections. For engineering reasons, it was most desirable to make the interstellar collector the same size and shape as the cometary collector. In so doing, one instrument accomplishes two sampling experiments. The number of interstellar particles collected is then primarily dependent on the length of the collection exposure period for this fixed collection area.

[47] Using the mean interstellar dust flux of $1.5 \cdot 10^{-4}$ per m^2 per s calculated from Ulysses data [Grün *et al.*, 1994], the number of interstellar particles expected to be collected for the surface area of 1037 cm^2 will be about 1.3 particles per day of exposure. It was felt that one tenth of the cometary objective; that is, 100 particles ($\beta = 1$) would be a reasonable target floor. This would require a minimum of about 77 days of interstellar collection.

[48] Unlike cometary collection, where particles can be easily distinguished from other sources due to their higher flux and highly collimated tracks, interstellar samples will be captured along with comparable fluences of sporadic IDPs and possibly β micrometeorites. Although the interstellar dust should be loosely collimated ($\pm 15^\circ$), at least for particles with the same β , the tracks of individual particles of different β will not be parallel within the aerogel. This will make it difficult to separate interstellar particle from

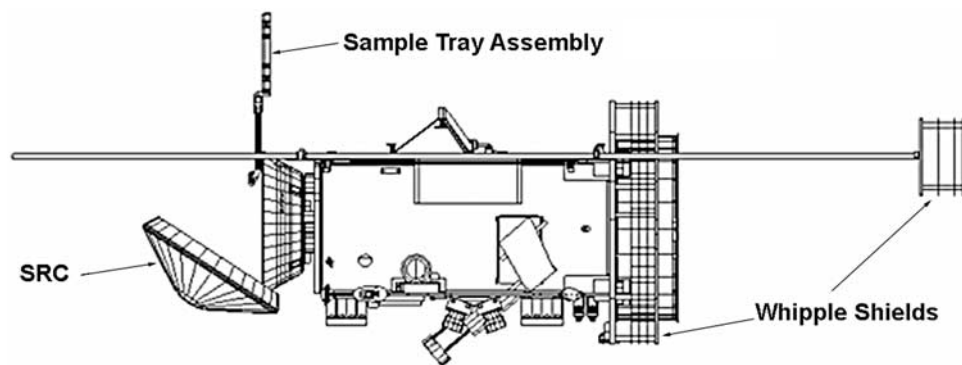


Figure 8. Sample Return Capsule mounted on the aft end of the spacecraft, showing STA fully deployed.

those of random IDP, β micrometeorites or embedded grains.

3.3. Instrument Objectives and Requirements

[49] With the above described considerations and project-level specifications [Brownlee *et al.*, 2003], WISCER has the following specific objectives and design requirements. These objectives and requirements were derived from the Stardust proposal [Brownlee *et al.*, 1994] and subsequently formalized in the Stardust Science Requirement Document (P. Tsou, unpublished data, 1996).

3.3.1. Instrument Objectives

[50] The instrument objectives were to (1) capture ≥ 1000 analyzable $15\ \mu\text{m}$ diameter particles from Wild 2; (2) capture $\geq 10^{15}/\text{cm}^2$ of cometary volatiles swept through Wild 2's coma; and (3) capture ≥ 100 analyzable interstellar dust particles in the $0.1\text{--}10\ \mu\text{m}$ diameter range.

3.3.2. Instrument Requirements

[51] The instrument requirements were to (1) capture Wild 2 samples with $\geq 1:5$ variable density ratio with aerogel capture medium $\leq 50\ \text{mg/ml}$ in density and $\geq 3\ \text{cm}$ in depth; (2) capture interstellar samples with $\geq 1:5$ variable density ratio with aerogel capture medium $\leq 20\ \text{mg/ml}$ in density and $\geq 1\ \text{cm}$ in depth; (3) fabricate aerogel capture medium with inorganic contaminants $\leq 100\ \text{ppm}$; (4) fabricate aerogel capture medium with carbon content $\leq 5\%$ by mass; (5) fabricate aerogel capture medium with $\leq 10/\text{cm}^3$ embedded grains $\geq 10\ \mu\text{m}$ in diameter; and (6) maintain capture medium cleanliness and physical integrity during all ground handling, Earth return, and postflight processing.

3.3.3. Project Requirements

[52] The project requirements were to (1) achieve a Wild 2 to collector relative encounter speed of $\leq 6.12\ \text{km/s}$; (2) target a nominal Wild 2 encounter distance of $150\ \text{km}$; (3) protect the WISCER from secondary debris during the Wild 2 encounter; (4) minimize in-flight exposure of the collector assembly to contaminants; (5) maintain the WISCER's cleanliness throughout ground handling and in flight; (6) qualify the actual flight aerogel by analogy; and (7) install the flight aerogel tray assembly at the launch site, Kennedy Space Center.

[53] Landgraf has made a prediction of the sample population that is expected to be captured by the WISCER [Landgraf *et al.*, 1999]. The exact nature of the

returned samples will only be revealed after their recovery in 2006.

4. Stardust Sample Subsystem

[54] The Sample Subsystem contains three sets of flight components: the Sample Return Capsule (SRC), the Sample Canister (SC), and the Sample Tray Assembly (STA). The WISCER is the portion of the Sample Subsystem directly related to the aerogel sample collection medium designed, fabricated, and installed by the JPL Media Development Laboratory (MDL) and integrated with the remaining Sample Subsystem by LMA.

4.1. Sample Return Capsule (SRC)

[55] The final Sample Subsystem design deploys the STA by opening the entire forward ablative shield of the SRC like a clamshell as shown in Figure 1. The baseboard of the SC is mounted on the back shell of the SRC and holds SRC's internal structure and electronics. During atmospheric reentry, the SC equalizes pressure with the ambient atmosphere by allowing air to enter through a vent filter. The STA is mounted at the end of an arm with two joints that allow the STA to be alternatively extended for collection and stowed for capsule reentry. The mechanisms within the SRC consist of two clamshell latches, one clamshell hinge, two wrist motors that deploy the STA, and associated gears. Each wrist motor can rotate 180° . Microswitches indicate the detent points for the clamshell hinge and wrist motors. These mechanisms are provided with heaters. Dual wind motor coils and duplicated heaters provide redundancy. The SRC measures $81.2\ \text{cm}$ in diameter and $49.9\ \text{cm}$ in height and executes its primary active function during Earth reentry. The $5.8\ \text{cm}$ thick front heatshield consists of phenolic impregnated carbon ablator, which absorbs and carries away the capsule's entry kinetic energy through ablation during atmosphere reentry. The backshell has a $1.0\ \text{cm}$ thick heatshield mounted like a clamshell with a hinge and locking mechanisms. The base of the backshell houses both drogue and main parachutes used to slow the descent of the capsule after the ablative reentry. A battery powers a beacon within the capsule to facilitate descent tracking. The SRC is expected to maintain the SC and the STA at temperatures less than 50°C during Earth atmospheric reentry and to bring the captured samples safely to the ground.



Figure 9. Photograph of the Sample Canister (SC), showing the base plate, the cover with center-mounted vent filter, and six of the eight temperature tapes.

[56] The SRC is mounted at opposite end of the rectangular Stardust spacecraft bus from the Whipple shields, as shown in Figure 8. Multilayered dust shields protect the spacecraft bus and solar arrays during Wild 2 encounter. The main shield also protects the STA mechanisms up to the base of the deployed STA.

4.2. Sample Canister (SC)

[57] The base of the SC is a 2.5 cm thick, nearly circular, 61.0 cm diameter, all aluminum honeycomb plate with aluminum face sheets as shown in Figure 9. The base serves as an anchor surface for the STA and SRC's related mechanisms. The mechanisms are those electro-mechanical devices needed to deploy the STA and to open, close, and lock the SRC clamshell. The inside canister face sheet is 0.08 cm thick 7075-T73 bare aluminum. The SC cover is a near circular 6061-T62 aluminum cover of 50.3 cm diameter and 10.2 cm height.

[58] A seal surrounds the edges of the SC to prevent inadvertent contamination penetrating to the STA. The teflon seal is U shaped and stiffened by a stainless spring. It is capable of maintaining a 1.0 psi differential pressure across the seal.

[59] The vent filter, located in the center of the SC cover (Figure 9), serves to equalize pressure within the SC during launch ascent and Earth reentry while traps the entry of contaminants. The filter is designed primarily to prevent ablated heatshield products from contaminating the collected samples during Earth reentry as the internal canister vacuum equalizes to atmosphere pressure. The filter, 6.4 cm in diameter, is designed to stop particles greater than 2 μm from entering the SC. The water and hydrocarbon filtrate material is activated carbon (Alfa/Aesar 88764) sandwiched between two electorate filters as shown in Figure 10. The electorate filtrate media is permanently charged rectangular polypropylene fibers made by 3M (G-0130). The capacity of the activated charcoal within the filter is sufficient to maintain the SC at less than 10% relative humidity and less than 15 ppm hydrocarbons for 20 days after landing. Eight temperature tapes are placed on the top and sides of the SC cover to monitor the temperature extremes experienced by the samples (Figure 9).

4.3. Sample Tray Assembly (STA)

[60] The STA consists of cometary and interstellar trays mounted back-to-back made with nonanodized aluminum (Figure 11). Each tray holds 130 rectangular and two trapezoidal aerogel capture cells. The STA is mounted at the end of a 2.5 cm diameter, 45.5 cm long tabular 6061-T6511 aluminum arm. The two trays are nearly identical except for the size of the two trapezoidal cells and their thickness (3 cm and 1 cm for the cometary and interstellar collectors, respectively).

[61] The probability of a hit of the STA by a large particle (1 mm to 1 cm in diameter) is calculated to be about 0.0009 (Table 1). However, a contingency for tray damage due to

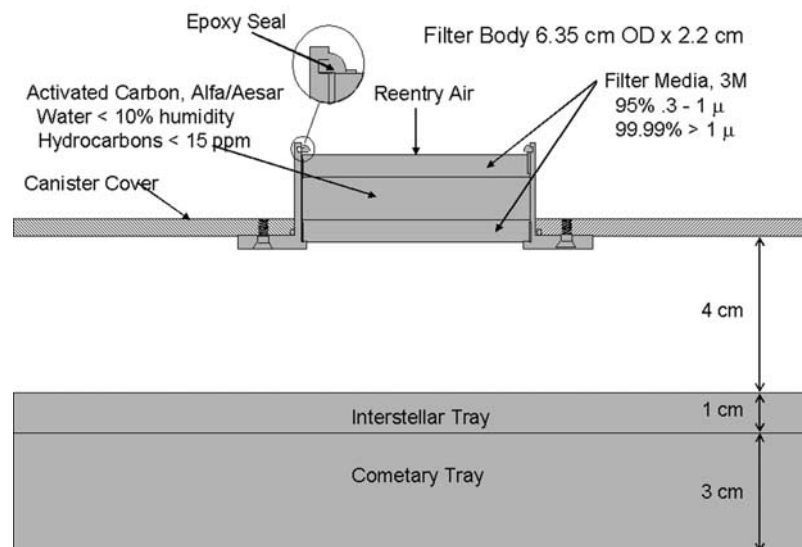


Figure 10. Sample Canister vent filter cross section and position with respect to the Sample Tray Assembly (STA) during launch and Earth return.

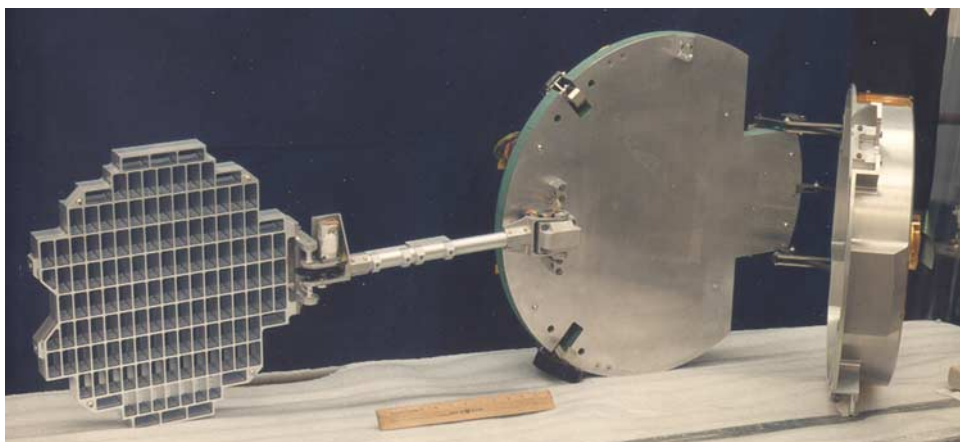


Figure 11. Photograph of the actual STA fully extended in the left and the opening SC on the right. The contamination control coupons are mounted on the STA arm next to the wrist motor housing.

large particle impacts has been considered in the tray design. By using brittle 6061-T6511 aluminum and the minimum cross sections in the tray frame members, a large particle impact will most likely damage the tray by sheering, thereby improving the chances that the damaged tray can still be stowed. Furthermore, the cometary and interstellar trays are aligned and there is no separator plate between them; large particles that miss the tray frames can punch through both sets of aerogel cells without damaging the trays themselves.

4.4. Aerogel Capture Medium

[62] The most critical components of the WISCER are the aerogel capture cells. As part of the flight hardware process, an Interface Control Document (ICD) was written to define the physical interface parameters of the capture cells with the sample trays [Ward et al., 1997]. The ICD also specified the qualification and acceptance test criteria for the aerogel.

4.4.1. Aerogel Capture Cell Shape and Size

[63] For practical reasons, it is desirable to have the aerogel capture medium consist of many small pieces. This localizes aerogel damage from very large particle

impacts and allows for ease of sample examination and distribution.

[64] Rectangular cells result in relatively good mechanical strength for the individual cells and provide a short optical path across one dimension for post flight particle detection and analysis. This size also conveniently allows the use of a standard quartz microscope slide as a base plate in handling and storage of aerogel cells. Cells were designed with four 0.635 cm rounded corners to minimize corner damaged during installation and removal from the trays and to allow a larger area cross section at the intersections among the sample tray frame.

4.4.2. Aerogel Cell Containment

[65] Aerogel cannot be attached to other materials by normal means (glue, screws, etc.) without severe damage to the aerogel, and several schemes have been used to hold it at JPL MDL, i.e., teflon cup and window frame [Tsou et al., 1993]. Aerogel can exhibit fairly elastic behavior for compressions less than ~10%, and this property was used to advantage in the mounting of the Stardust aerogel cells via wedge containment (Figure 12). This containment concept greatly simplifies the tray design with only one component; that is, one tray, for minimal mass, eliminates

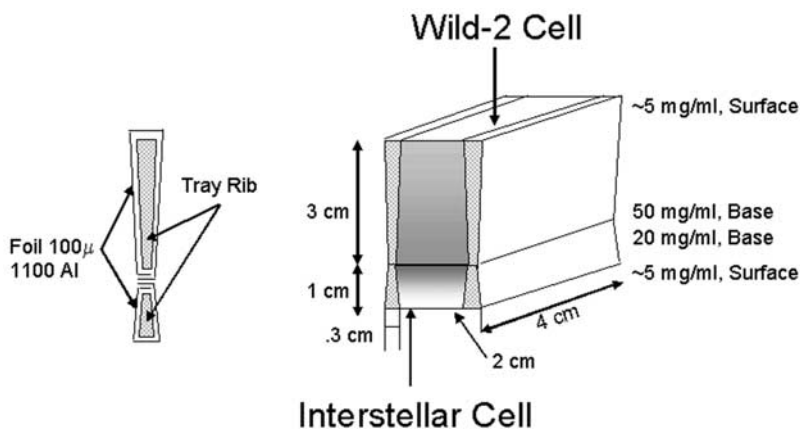


Figure 12. Cross-sectional view of the aerogel capture cells contained by two opposing wedges. The left-hand cross sections show the tray wall frames with wrapped aluminum foils.

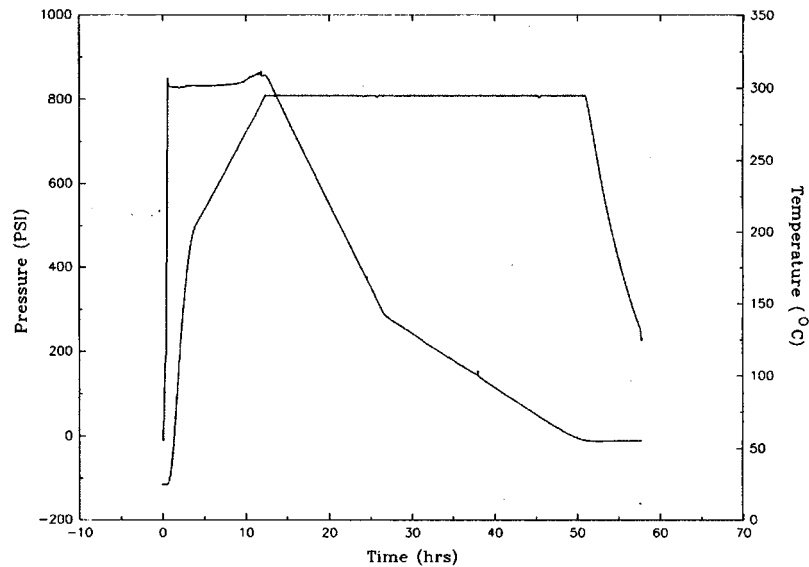


Figure 13. Typical supercritical critical point extraction temperature-pressure-time profile for an entire batch run.

the need for a base plate between the cometary and interstellar trays, and effectively allows each tray to “extend” the capture range of the other tray.

4.4.3. Aerogel Cell Types

[66] As discussed in section 2, the initial shock pressure experienced during impact by hypervelocity particles correlates directly with the density of the target material for a given mesostructure. Consequently, it is highly desirable for an aerogel capture cell to have the lowest possible density at the particle entry surface. A monolithic ultra low-density aerogel cell would present low shocks but has to be very thick to stop a large particle. Ideally, one would fabricate a capture cell in which the aerogel density is low at the entry surface and increases along the direction of penetration. This would reduce the overall required aerogel thickness to stop a given sized particle while minimizing the shock pressures on impact and present commensurate reduction of shock pressures.

[67] To ensure meeting the flight fabrication schedule, a Stardust Aerogel Workshop of aerogel experts from US and Europe was convened in 1996 to elicit techniques for variable density aerogel fabrication. Toward this, several techniques to fabricate variable densities were developed at JPL MDL for Stardust. The first successful variable density aerogels was layer density cells; that is, each cell consisted of stacked layers of aerogel of lower densities. Later, aerogel cells having a continuous density gradient were developed. The basic chemical processes used to fabricate both the layered and continuous density aerogels was the same two-step sol-gel process.

[68] Two types of layered density aerogel formulations, designated as C1 and C2, were selected to accommodate

fluffier and solid particles in the cometary tray. Only one formulation, I, was designated for cells in the interstellar tray. The cometary cells had three density layers; the interstellar cells had only two. Table 2 summarizes the target density profiles of the different layered density cell types.

[69] Several approaches including centrifugation were explored for generating continuous gradient density aerogel. The final process was found to be one similar to that used to make variable concentration sugar media. Density of monolithic aerogel can be measured by weight/volume. Density does vary from cell to cell and batch to batch due to manual processing and shrinkage variability introduced by the supercritical extraction process. For variable density aerogel, a nondestructive technique for measuring aerogel density must be developed. The new technique makes use of optical refraction to measure densities. The index of refraction (n) of aerogel is density (ρ [mg/ml]) dependent, $n-1 \approx 0.21\rho$. The density of an aerogel cell is measured by illuminating the corner of the cell with a narrow sheet of laser light and measuring the profile of the refracted light. This process was calibrated by the amount of light refraction produced by known density aerogels. Generally the density ratios of the variable density aerogels were found to range from 1:5 to 1:10 (the surface: base aerogel density ratio).

4.4.4. Aerogel Fabrication

[70] Although silica aerogels can be made quite transparent, the ability to optically examine small features buried within them is best to about 1 cm in depth. The optical quality of aerogel surfaces, in order of decreasing quality, is: cleaved, cast, and cut. Cleaved aerogel provides the best optical surface, but aerogel cannot not be cleaved precisely.

Table 2. Target Density Profile of Different Stardust Layered Aerogel Cells

C1		C2		I	
Thickness, mm	Density, mg/ml	Thickness, mm	Density, mg/ml	Thickness, mm	Density, mg/ml
15	5	7	5	2	2
5	30	8	30	8	20
10	50	15	50		

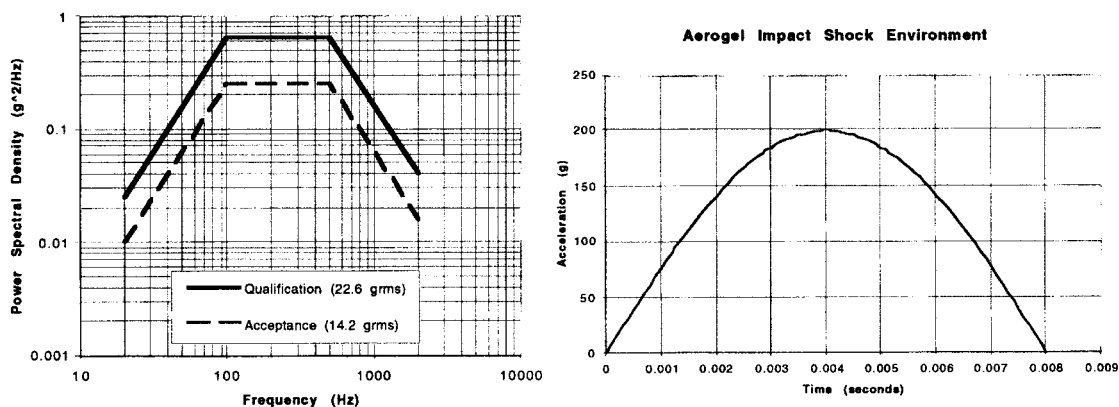
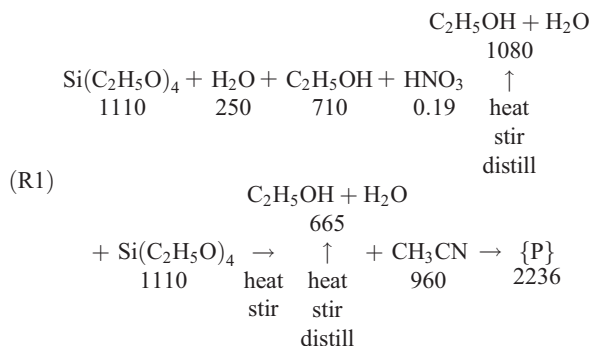


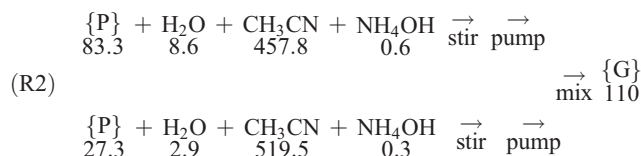
Figure 14. Aerogel capture cells (left) vibration and (right) shock qualification test profiles.

Physical shaping with a blade or laser yields poor optical surfaces and has the additional disadvantage of producing large numbers of silica or glass debris. Cast surfaces render acceptable optical surface if the fabrication mold is smooth and the surface well prepared. Casting also generates a $\sim 1 \mu\text{m}$ thick protective "skin" that minimizes damage during handling. Consequently, casting aerogel into the desired cell dimensions without further shaping was the fabrication approach chosen for Stardust.

[71] The Stardust silica aerogels were fabricated by the two-step sol-gel process [Hrubesh, 1989] followed by high temperature supercritical point extraction and a mild vacuum-bake cycle. The two-step gelation process provided distinct advantages: (1) the ability to fabricate ultra low-density aerogels; (2) the ease of making a single precursor to minimize batch to batch precursor variations; and (3) the ability to make varying density aerogels at the time of the final mix. This high temperature supercritical point extraction resulted in aerogel of high transparency ($>95\%$ @ 800 nm), pure quality (inorganic < 100 ppm), and high yields ($>90\%$). The gel precursor {P} was generated using commercially available tetraethylorthosilicate [$\text{Si}(\text{C}_2\text{H}_5\text{O})_4$]. Aldridge's 98% grade was used after further distilled through a 12 stage Schneider column to reduce organic impurity. A partially hydrolyzed $\text{Si}(\text{C}_2\text{H}_5\text{O})_4$ was then produced with a substoichiometric amount of H_2O via acid catalysis. Then hydrolyzation was arrested with CH_3CN dilution as illustrated in process flow reaction (R1). The production of a single large batch of the $\text{Si}(\text{C}_2\text{H}_5\text{O})_4$ precursor was sufficient to fabricate the entire flight inventory. The quantities below the listed reagents show typical volumetric amounts in ml for the precursor (reaction (R1)) and gelation (reaction (R2)) processes.



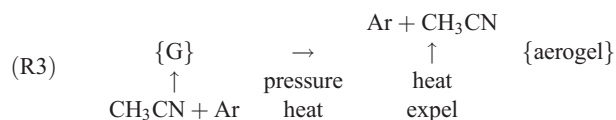
[72] The next step of the sol-gel process completes the hydrolysis by adding water and dilutant with base catalysis to enhance gelation in a mold, as shown in process flow reaction (R2). The interlinking of the initial silicon dioxide clusters during the gelation process does not usually run to full completion. These unlinked individual cluster centers accumulate into micron-scale or larger grains within the aerogel. These incorporated SiO_2 grains can be confused with captured particles; thus the precursor mix was filtered through a $1 \mu\text{m}$ pores membrane before casting to reduce these embedded grains. An extracted aerogel made using this procedure was measured to have <10 micron sized clusters/ cm^3 . Further filtering can remove more clusters but can also result in immediate gelation.



[73] Gelation occurs in a three piece mold consist of a base, a four-sided ring, and a cover plate fit inside the ring. Quartz molds were used to minimize inorganic contamination during critical point extraction. A silicone mold release was used to prevent the aerogel fusing to the mold. Silicon was used as a sealant between the ring and the mold base. After pouring measured final mix into the sealed molds, they are placed in a glovebox at room temperature with a saturated CH_3CN solvent to complete the crosslinking into a monolithic gel. For layered gradient density cells, successively lower density batches of mixture were poured on top of the previously gelled layer within the same mold. For continuous gradient density cells, two batches of high, e.g., 50 mg/ml, and low, e.g., 5 mg/ml, and density mixtures were made, pumped, and mixed with a peristaltic pump into the prepared molds to allow crosslinking and polymerization into a single monolith gel {G} shown in reaction (R2). The profile of the density gradient depended on the pumping rates from the high and low-density batches of mixes.

[74] Once gelled, the cover was placed over the gel and the mold placed into an autoclave where the cells were supercritically extracted as shown in reaction (R3). A typical supercritical extraction pressure/temperature/time profile is shown in Figure 13. Supercritical extraction in

the autoclave breaks the silicon seal, leaving the aerogel free for removal from the mold.



[75] All reagents used for the production of the flight aerogels were purchased from a single lot and monitored by GC/MS to document the organic contents and by ICP/MS for the inorganic content. After extraction, the aerogel cells were baked for 72 hours at 300°C to reduce their carbon content to <2% by mass. A controlled flow of filtered air at 5–6 psi was flowed through the furnace during heating. Twice a day the flow of air was stopped and the furnace was evacuated to <10 torr for 30 min.

[76] In order to ensure quality control for each aerogel processing step, instruments were selected to provide quantitative monitor of process parameters. Fast Fourier infrared spectroscopy and gas chromatography mass spectrometry provided monitoring of the organic composition and purity of reagents before and after distillations. A refractometer particle counter was used to assess the size of particulates in the sol to judge the amount and number of cluster centers. Thermal Graphic Analyzer/Mass Spectrometry was used to measure the amount of surface depositions in the aerogel. A UV Vis Spectrometer provided the degree of transmission through the aerogel cells from the UV to near IR. An Instron was used to measure the mechanical properties of the various aerogel formulations. Finally, Caltech's Neutron MR was used to examine precursor mixes and an Inductively Coupled Plasma Emission Spectroscopy (ICP/MS) proved to be most useful for characterizing the inorganic compositions of the aerogels.

4.4.5. Aerogel Insertion Into and Removal From the Sample Trays

[77] Aerogel capture cells were secured in the collection tray cell cavity by compression with the low-density side of the cell sustaining the highest compression of ~8%. To allow for a nondestructive method of cell removal by not having to press on the low-density face of the aerogel cell, 102 μm thick 1100 aluminum foils surround the four aluminum tray cavity walls. This allows the cell to be removed by pulling on the foils from the backside of the capture cell without having to press on the low-density entry surface. This aluminum foil wrapping scheme is shown in Figure 12. Individual foil pieces were cut with a rotary blade into two 3.2 and 1.2 cm widths from a roll of 1100 aluminum foil. Then on a jig, the strips were cut into 7.5 and 3.5 cm lengths for cometary and interstellar cells, respectively. The long and short cell removing aluminum foils were all placed individually on the tray frame webs before aerogel cells were inserted. The trays contain a total of 146 long foils covering the 4 cm cell sides, and 150 short foils for the 2 cm cell sides. The exposed surface area for the long and short sides are 1.3 cm × 0.23 cm and 3.3 cm × 0.23 cm, respectively, providing a total exposed foil surface area of 153 cm² on both the comet and interstellar facing direction. This is about 15% of the total exposed aerogel surface area and provides an excellent capture medium for small solid particles.

4.4.6. Aerogel Contamination Control

[78] Contamination of the aerogel is obviously undesirable, but not completely avoidable. Aside from the contamination introduced during aerogel ground operations (fabrication, processing, assembly, and examination), contamination could be introduced during the flight tray transportation from JPL to LMA, sample tray installation, flight system testing, transporting to KSC, launch, encounter, Earth atmosphere reentry, and ground processing after Earth return. To this end, three Stardust contamination management processes were developed: a Spacecraft Contamination Control Plan, SD-60000-110 (including specifics on the WISCER), an Aerogel Fabrication Contamination Control Plan (D. M. Taylor, unpublished data, 1998), and a Sample Return Capsule Recovery Operations Plan (M. S. McGee, unpublished data, 1998). All flight hardware, including the STA and the transport case, were cleaned according to JPL flight hardware cleaning procedure, FS505146E. The key cleaning solvent used was Freon 11. The aluminum foils were also cleaned by the same hardware cleaning process.

[79] The possible sources of contamination fall in three groups: (1) process, when chemical impurities bonded as part of the aerogel internal structure; (2) handling, when impurities trapped by the aerogel, either gaseous or particulate contamination; (3) flight, when impurities introduced during flight, such as spacecraft outgassing, dustshield secondary debris, or reentry heatshield ablation products.

[80] The aerogel fabrication process can introduce both process and handling contamination. Inorganic impurities in the reagents will become part of the aerogel structure. The tetraethylorthosilicate supplier was selected among six reagent vendors. Reagents such as ethanol and acetonitrile were further distilled with a high efficiency Schneider column. JPL's water purifying plant built for the JPL Microdevices Laboratory supplied water for the process. Reagent grade catalysts were used without distillation. Sufficient quantities of reagents for the entire fabrication effort were purchased from one lot to ensure purity control and consistency. All aerogel molds, processing glassware and surfaces in contact with flight aerogel were made with quartz to reduce possible inorganics leaching into the reagents or aerogel.

[81] The second highest source of process contamination is handling aerial deposits into the reagents before solvent extraction on aerogel cells. This contamination source was minimized by equipping the JPL MDL with both dust and hydrocarbon and particulate to Class 5,000 and for selected critical areas to Class 100 in tents. The aerogel insertion and examination were carried out in Class 100 tent to minimize contamination. A special glove box was fabricated at LMA to integrate STA into SC and the SRC during STA deployment tests.

[82] The SRC is located aft of the dust shields. The principal source of flight contamination will likely come from secondary debris generated by impacts on these dust shields. The sides of the multilayer dustshields have been enclosed to minimize secondary plasma plume debris escaping the shields. Molecular contamination from the hydrazine used for the attitude control thrusters was minimized by placing the four thruster pods at the opposite side of the spacecraft away from STA. The gaseous condensation of various spacecraft components was minimized by delay-

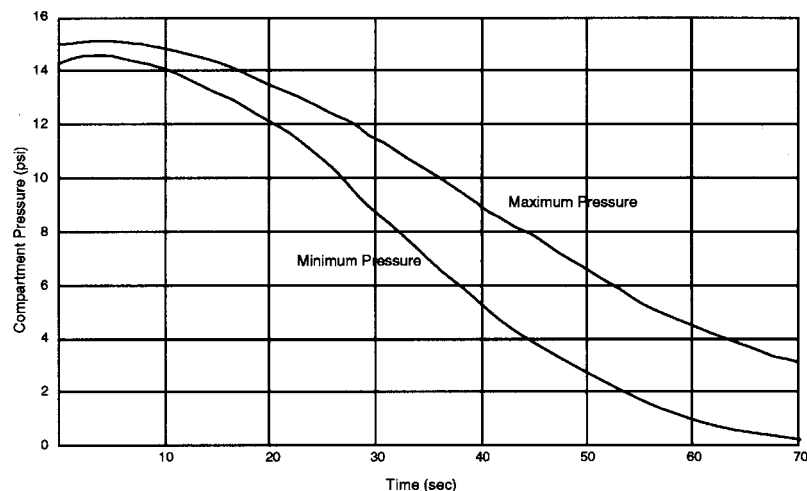


Figure 15. Aerogel pressurization/depressurization test profiles.

ing opening of the SRC after launch until the spacecraft had time to outgas.

[83] To assess in-flight contamination of the captured samples, contamination control coupons (CCC), aluminum and sapphire disks and an interstellar aerogel cell, have been mounted on the STA deployment arm just below the view of the Wild 2 samples. These coupons should be exposed to all the same source of contamination as the flight tray cells, but will not be exposed to Wild 2 particles.

5. WISCER Qualifications

[84] The flight qualification process for the WISCER included both engineering and scientific tests. Qualifications are necessary in validating and uncovering faults in designs. Engineering qualifications were performed by LMA and JPL engineers and scientific qualifications performed by Stardust sample Co-Investigators.

5.1. Engineering Qualification

[85] The key engineering tests concerning WISCER were the qualifications of the method of aerogel containment and the integrity of aerogel cells contained in STA under launch and landing environments. Of the many engineering qualification tests performed, only three are directly pertinent to WISCER.

5.1.1. Aerogel Cell Qualifications

[86] A generally desired characteristic of space flight hardware is robustness. Aerogel, on first impression, is not a particularly strong material, and it was necessary to carry out a number of tests designed to gain confidence for the LMA engineers in the survivability of aerogel for flight. Initial tests were made on single cell jigs of 4×4 cm, 2×8 cm and 2×4 cm mono-density aerogels having thickness of 3 cm and 1 cm and densities ranging from 10 to 60 mg/ml. These were performed at the LMA's Material Test and Acoustic Vibration Laboratories and the Metrology Laboratory of University of Colorado. Tests included standard compression tests, three point bending tests, shear tests, creep tests, centrifuge tests up to 150 G, and random vibration tests. The aerogel, even those that had previously impacted at ~ 6 km/s with 100-

270 μm FeS beads at the NASA AVGR, held up extremely well [Rogers, 1996]. Indeed, the primary failures during these tests were the result of handling by test personnel! After these tests, the LMA engineers were convinced that the WISCER did not need to be specially shock mounted resulted in a significant reduction in complexity and mass.

[87] The first qualification tests of layered density flight aerogel capture cells occurred on 1 September 1997. The qualification test levels were set higher than expected launch vibration and landing shocks to provide safety margins. Owing to successful extensive containment qualification tests, only random vibration and pyro shock qualification tests were judged necessary for representative qualification for newly fabricated aerogels. The levels and profiles for these tests are shown in Figure 14.

[88] The first qualification test of 15 cometary and 15 interstellar aerogel capture cells of the same formulation inserted manually into the qualification holder with removable aluminum foils was a success. No aerogel cell fell out the test holder and none suffered any significant damage. Second and third qualification tests of the layer capture cells were carried out on 5 January 1997 and 1 May 1998, respectively. These consisted solely of pyro shock tests. Both shock tests were uneventful and no aerogel damage was observed. The first continuous gradient density aerogel cells were tested in June 1998. Both launch vibration and pyro shock tests were passed without incident and the aerogel cells were fully qualified for flight.

5.1.2. Aerogel Evacuation/Repressurization Tests

[89] Aerogel is open cell foam and as a result it will undergo one complete depressurization to vacuum at launch and one repressurization to 1 atm on Earth return. Aerogel depressurization and pressurization qualification in the 3×5 cell qualification holder fill with both flight cometary and interstellar aerogels were performed at JPL's Environmental Laboratory [Martin, 1998]. The pressure time profiles are shown in Figure 15. Substantial clouding resulted in the chamber during depressurization due to outgassing of moisture trapped in the aerogel cells, but this moisture quickly sublimed and no visible damage was detected in

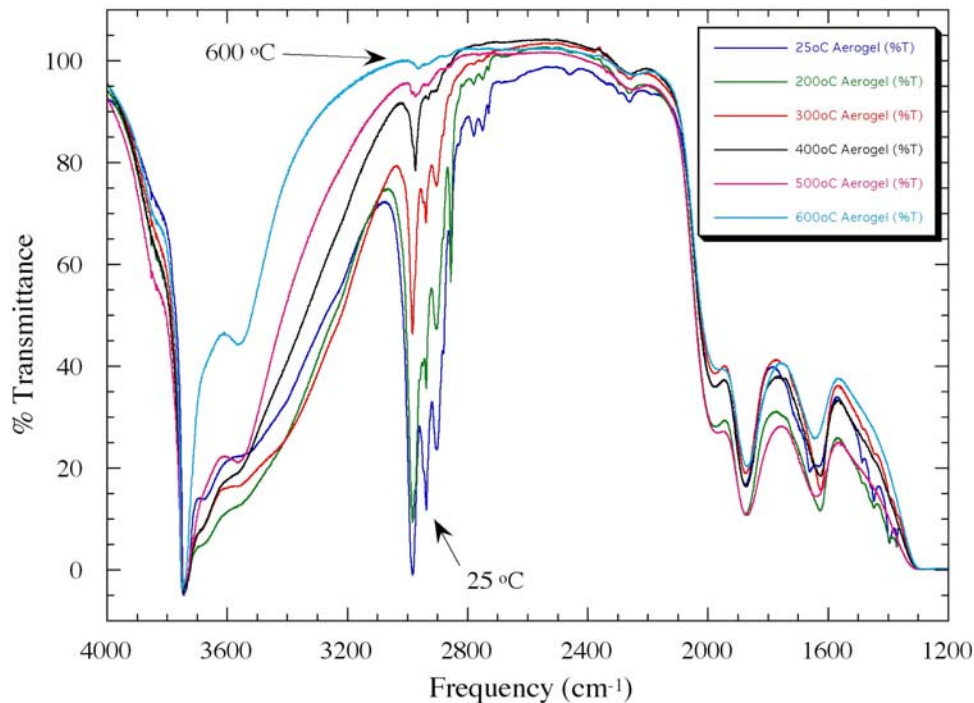


Figure 16. Aerogel IR absorption spectra for baking at increasing high temperatures. At 600°C, most of the organics will be removed, but significant aerogel shrinkage would occur.

the aerogel in either the evacuation or the repressurization tests.

5.1.3. Sample Subsystem Qualifications

[90] Three tests were performed to qualify the Sample Subsystem: (1) an SRC subsystem drop test from a moving truck, designed to assess the integrity of the capsule and canister design and to measure the acceleration level expected with a horizontal wind; (2) a thermal/vacuum test of the entire spacecraft to qualify the thermal and vacuum performance, including exercising the mechanism in extending and retracting the sample tray filled with aerogel; and (3) a balloon drop test from 84.2 km for the operation of the parachutes and the separation of the parachutes on landing. All tests were successfully passed.

[91] A final engineering development unit of the complete Sample Subsystem was also dropped twice with full 133 aerogel cell loaded trays (uniform density aerogel: 50 mg/ml for the cometary cells and 20 mg/ml for the interstellar cells). No damage was found in the aerogel.

5.2. Scientific Qualification

[92] Validating the scientific aspects of the design encompasses the determination of the compositional purity of the flight aerogel, the efficacy of the intact capture in the flight aerogel capture cells, and the effectiveness of the SC filter to control contamination to the captured samples. Previous tests of the ability of aerogel to capture hypervelocity particles had all been made with mono-density aerogel. It was therefore necessary to verify that the layered and continuous gradient density aerogel cells made for Stardust worked as well as, or better than, monolithic density aerogel.

5.2.1. Aerogel Capture Efficacy Validation

[93] A series of capture evaluation experiments were performed at the Johnson Space Center (JSC) two-stage

light-gas gun with various densities of aerogels provided an independent and systematic data of intact captures in mono density aerogels [Hörz *et al.*, 1998]. The projectiles used included aluminum, aluminum oxide, glass, olivine, pyrrhotite, Allende, Pampa, and coca powder. Projectiles were launched into 10, 20, 35, 40, and 50 mg/ml single density aerogels fabricated at JPL MDL. These experiments established systematic baseline of intact capture of all these types of projectiles in mono-density aerogel at impact speed of 6 km/s. Similar tests were then performed on both layered and continuous gradient density aerogel cells. In all cases, the projectiles were recovered in similar conditions. The continuous gradient density aerogels appear to produce no more damage to the particles than comparable single density aerogels, while result in shorter tracks. Thus the density gradient aerogel does not compromise sample survival efficiency while decreasing the total thickness of the cells and increasing the maximum particle size that can be captured in a given aerogel thickness.

[94] Validation tests were performed at the AVGR with cluster shots. Each cluster shot impacted four targets (mono-density, layered density, continuously variable density, and baked continuous variable density) with the same mix of projectiles. For cometary cells, 50–150 μm sized mixture of glass, olivine, and FeS projectiles were used. Individual 4–6 μm diamond grains were launched into interstellar cells. No adverse effects were detected with either layered or continuous gradient density aerogel.

5.2.2. Aerogel Organic Contamination Analyses

[95] Several analytical methods were used to assess the organics entrapped in the aerogel cells. These included Vacuum Graphic Analysis (VGA), Thermogravimetric Analyzer/Mass Spectrometry (TGA/MS), Infrared (IR)

Table 3. Inorganic Composition of Stardust Aerogel by ICP Concentration^a

	Detection Limits, ppb	Detected Concentration, ppb
1 Aluminum (Al)	2	2460
2 Antimony (Sb)	1	3.8
3 Arsenic (As)	5	<5
4 Barium (Ba)	1	52
5 Beryllium (Be)	3	<3
6 Bismuth (Bi)	1	1.5
7 Boron (B)	10	1900
8 Cadmium (Cd)	1	1.9
9 Calcium (Ca) ^b	10	5200
10 Cerium (Ce)	1	1.2
11 Cesium (Cs)	1	<1
12 Chromium (Cr)	3	38
13 Cobalt (Co)	1	1.5
14 Copper (Cu)	2	182
15 Dysprosium (Dy)	1	<1
16 Erbium (Er)	2	<2
17 Europium (Eu)	2	<2
18 Gadolinium (Gd)	2	<2
19 Gallium (Ga)	1	<1
20 Germanium (Ge)	2	1500
21 Gold (Au)	5	<5
22 Hafnium (Hf)	5	<5
23 Holmium (Ho)	1	120
24 Iridium (Ir)	5	<5
25 Iron (Fe) ^b	10	1800
26 Lanthanum (La)	1	<1
27 Lead (Pb)	2	300
28 Lithium (Li)	2	10
29 Lutetium (Lu)	2	<2
30 Magnesium (Mg)	2	2000
31 Manganese (Mn)	3	30
32 Mercury (Hg)	50	<50
33 Molybdenum (Mo)	2	2.7
34 Neodymium (Nd)	2	<2
35 Nickel (Ni)	3	88
36 Niobium (Nb)	2	2.1
37 Osmium (Os)	2	<2
38 Palladium (Pd)	5	<5
39 Phosphorus (P)	200	<200
40 Platinum (Pt)	5	<5
41 Potassium (K) ^b	5	870
42 Praseodymium (Pr)	1	<1
43 Rhenium (Re)	2	<2
44 Rhodium (Rh)	1	<1
45 Rubidium (Rb)	1	1.5
46 Ruthenium (Ru)	3	<3
47 Samarium (Sm)	3	<3
48 Scandium (Sc)	5	<5
49 Selenium (Se)	200	<200
50 Silver (Ag)	2	<2
51 Sodium (Na) ^b	5	5800
52 Strontium (Sr)	1	35
53 Sulfur (S)	2000	<2000
54 Tantalum (Ta)	2	<2
55 Tellurium (Te)	2	<2
56 Terbium (Tb)	2	<2
57 Thallium (Tl)	2	<2
58 Thorium (Th)	2	<2
59 Thulium (Tm)	1	<1
60 Tin (Sn)	1	28,000
61 Titanium (Ti)	5	148
62 Tungsten (W)	2	<2
63 Uranium (U)	2	<2
64 Vanadium (V)	1	2.3
65 Ytterbium (Yb)	2	<2
66 Yttrium (Y)	2	8.1
67 Zinc (Zn)	3	1,300
68 Zirconium (Zr)	1	151

Table 4. Input Gas Mixture for the Vent Filter Organics Absorption Test

Gas	Component Concentration, mbar					
	Test 1	Test 2	Test 3	Test 4	Test 5	Test 6
N ₂	0	845	845	950	790	955
C ₂ H ₆ O (ethanol)	10	50	50	0	50	7
CO	1	5	5	1	5	2
H ₂ O	0	0	0	0	0	15
C ₃ H ₆ O (acetone)	10	50	50	0	47.5	7
C ₆ H ₁₄ (hexane)	10	50	50	0	47.5	7
C ₆ H ₆ (benzene)	0	0	0	50	42.5	7

Spectroscopy, Gas Chromatography/Mass Spectrometry, and CHNS/O Analysis.

[96] Early IR provided evidence of the types of organics in the aerogel. This material was largely aliphatic-rich and CH₂-rich, suggesting that it consisted largely of ethyl groups within the structure of the aerogel. VGA at 10⁻¹ torr indicated that this aerogel surface trapped material amounted to about 2.4% of the total aerogel. Both IR and TGA/MS measurements demonstrated that this material, along with residual solvents, could reduce by mild heating. Heating the extracted aerogel from 200°C to 600°C yields the reduction of organics as shown in Figure 16. All the flight aerogel cells were subjected to 72 hours of heating at 300°C (see section 4.4.4) since physical shrinkage begins above 300°C. The most reliable method to measure the total amount of organic material in aerogel was the measurement of total carbon content with a Perkins Elmer PE 2400 Series II CHNS/O Analyzer by oxidizing the sample in pure O₂ environment. The gases generated in this manner were separated in a stepwise fashion and detected as a function of their thermal conductivities. The carbon content of the near flight like aerogel after baking to 300°C was found to be <0.5% by mass.

[97] The concerns for possible organic contamination from the mold release agent and silicon mold sealant were explored by analyzing the materials and tracing them in the final product. No significant amounts were detected from the final product aerogel [Sandford, 1997b].

5.2.3. Aerogel Inorganic Compositional Purity

[98] The inorganic purity of the aerogels depended primarily on the purity of the tetraethylorthosilicate reagent. Techniques used to ascertain the inorganic composition of the aerogel included Instrumental Neutron Activation Analysis (INAA), Synchrotrons X-Ray Fluorescence (XRF), TOF-SIMS, and Inductively Coupled Plasma Emission Spectroscopy (ICP/MS). These analyses demonstrated that the Stardust aerogel contains very little in the way of inorganic contaminants, even compared favorably to silicon wafers manufactured for the semiconductor industry [Tsou et al., 1994].

[99] INAA measurements of a 1 gm piece of aerogel detected Na (10 ppm), Fe (6 ppm), Br (0.2 ppm), Au (0.97 ppm), Co (0.002 ppm) and traces of Cr, An, Sb, Zr,

Notes to Table 3

^aMeasured in ppb (ng/g). The aerogel was digested with ultrapure HF to remove silicon, and the trace metals are stabilized by ultrapure nitric acid prior to ICP-MS analysis.

^bAnalyzed by GFAAS or Cold Plasma ICP-MS. All other elements were analyzed by hot plasma ICP-MS.

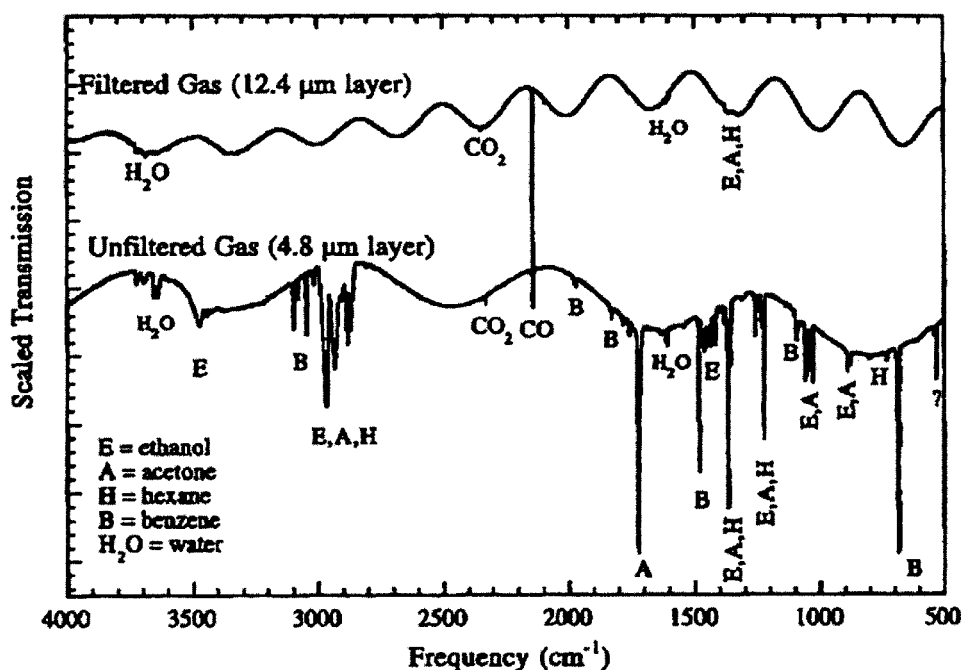


Figure 17. Comparison of the IR spectra of an organic-rich gas mixture before and after passage through the SC vent filter.

Hf, Ta, Cs, Ag, and As [Lindstrom, 1996] with the total being much less than 100 ppm. XRF analyses performed at Brookhaven National Laboratory for additional elements yielded similar results: Zn at 10 ppm, Cu a bit less, and Fe much lower (G. J. Flynn, personal communication, 1997). ICP/MS provided the most comprehensive analysis of inorganic contents on the flight batch aerogel and these are summarized in Table 3 [Tan, 1999].

5.2.4. Aluminum Foil Purity

[100] The 1100 aluminum foil serves both an engineering function for cell removal and a science function for capturing small particles on both the cometary and the interstellar sides. To ensure the purity of the foil, measurements were made with the quadrupole mass spectrometer at Washington University McDonnell Center which showed that the aluminum foil is indeed pure and quite clean (C. M. Hohenberg, personal communication, 1998).

5.2.5. Canister Vent Filter Performance

[101] The SC filter was subjected to a number of engineering and scientific tests. LMA performed engineering tests to evaluate the throughput and environmental performance of the filter. The filter's ability to absorb organic compounds including water and particulates, were performed at the NASA-Ames Research and NASA-Johnson Space Centers, respectively.

5.2.5.1. Filter Throughput Tests

[102] The original SC filter contained Gilman membrane molecular sieves placed on both sides of the activated carbon (Figure 10). However, tests made at LMA demonstrated that flow rate through the filter was too restrictive to accommodate the canister's decompression profile at launch. As a result, the sieves were removed to increase maximum possible flow rate. Two 18-8 stainless steel wire grids were added to contain the filtrate, provide thermal protection for the filtrate, and serve as a sunshade to prevent

possible UV damage to the filtrate media. The wire grids also serve as air diffusers.

5.2.5.2. Filter Organics Absorption

[103] The SC filter's ability to absorb organic compounds was tested by flowing known mixtures of gaseous organics through the filter and comparing the composition of the original and filtered gases using standard infrared matrix-isolation techniques. A total of six tests were performed from 1997 to 1998 to assess the performance of the filter [Sandford, 1997a, 1998]. The gas mixtures used for these tests are summarized in Table 4. The trapping efficiency of the filter for volatile organics was found to be ~98% for high loads and 99+% for lower loads. Figure 17 shows the infrared spectrum of one of the starting mixtures compared to the resulting filtered gas. The presence of water vapor was observed to have little effect on the filter's absorption of volatile organics. The filter was observed to release a small portion of the absorbed volatiles if it was subsequently depressurized. The tests indicated acceptable performance of the SC filter.

5.2.5.3. Filter Water Absorption and Particulates Trapping

[104] The filter's water absorption capacity and particulate trapping efficiency were tested at JSC. The water capacity was tested with 100% humidity air at 1 L/min

Table 5. Canister Filter Performance Tests (Humidity Trapping Test)

Amount of Air Through the Filter, L	Trapping Efficiency (at 100%), %	Trapping Efficiency (at 40%), %
0-10	75	91
10-20	71	96
20-30	65	88
30-40	74	87

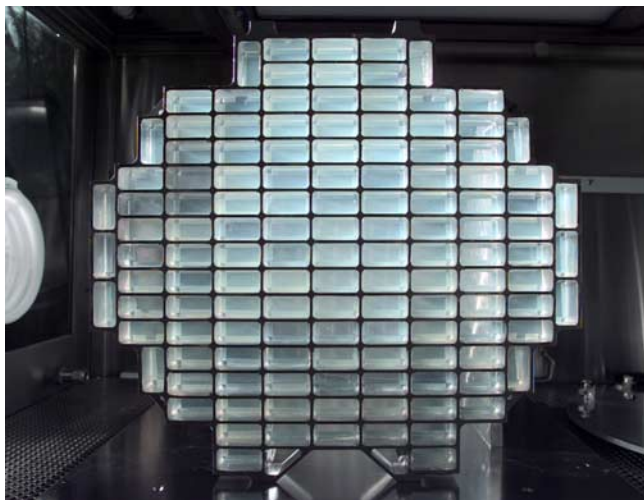


Figure 18. Wild 2 and Interstellar Sample Collection and Earth Return (WISCER) instrument loaded flight STA.

until either the filter was saturated or had passed 15 liters (approximate SC capacity) of 100% humidity air. As a test of the filter's ability to trap particulates, a test was also carried out in which 15 liters of cigarette smoke were passed through the filter. The results of particulate trapping efficiency test showed 99.9% efficiency over 0.3–25 μm particulates. The water absorption test results are summarized in Table 5 [Zolensky, 1997].

[105] These tests exceed the expected conditions that the filter will be exposed to during reentry and the filter's performance was deemed to be satisfactory.

6. Flight WISCER

[106] It took approximately 5 months from the time of the continuous gradient aerogel qualification to having produced sufficient flight quality aerogel capture cells to install into the flight and backup trays, to assemble, and to deliver the trays to LMA for integration with the Sample Subsystem. The final completed flight and spare tray assemblies were filled with 132 cometary and 132 interstellar, mostly continuous gradient density aerogel capture cells. These

were delivered to LMA in October 1998 where they were integrated into the SC then the SRC and spacecraft before the system level tests, then transported to Kennedy Space Center for launch on 7 February 1999.

[107] Owing to the inability to perfect casting the exact physical dimensions in cells, the flight aerogel inventory were filled by making large quantities of cells and “cherry picking” the best available. Up to 56 cometary cells or 84 interstellar cells could be fabricated in each production batch and ultimately cells from more than 46 total production batches were completed for the flight and backup tray inventory.

[108] A flight STA set and a backup STA set were assembled at the JPL MDL. Table 6 summarizes the fabrication trail of the mix of cells used to populate each of the flight trays. Figure 18 shows the final assembled flight tray. Each of the STA consists of one cometary tray filled with 132 cometary aerogel cells and one interstellar tray filled with 132 interstellar aerogel cells. The flight STA was completed for delivery on 26 October 1998 and the backup STA was completed for delivery on 27 March 1999. Earlier assembly made more use of layered aerogel cells and later assemblies were all of the continuous gradient density cells. Table 6 lists the pertinent aerogel production trail for the aerogel cells for the flight trays:

[109] The assembled STA was transported in a specially designed transport case from JPL to LMA. The all-aluminum transport case was sealed with an O-ring and the cover was held to the base plate with 30 bolts. A dry N_2 purge at 0.25 psi was maintained during transit.

[110] In order to protect the aerogel cells from the high humidity and salty atmosphere at the Kennedy Space Center, a septum was installed in the SC so that a tube could be connected to a continuous dry N_2 purge. This purge was maintained after the STA was integrated to the spacecraft and continued on top of the Delta II launch rocket. The tube was removed before launch.

7. Instrument Operations

[111] The WISCER fulfills the sample collection function passively without requiring any real-time commands. However, the engineering operations of the Sample Subsystem

Table 6. Aerogel Cells for the Flight Sample Tray Assembly

Cometary Flight Tray			Interstellar Flight Tray		
Type	Batch	Number of Pieces	Type	Batch	Number of Pieces
CGD	227	1	CGD	223	8
CGD	232	4	CGD	234	4
CGD	234	25	CGD	233	8
CGD	235	31	CGD	238	31
CGD	236	27	CGD	243	10
			layered	201	1
			layered	204	13
			layered	206	2
			layered	209	2
			layered	211	2
			layered	219	8
			layered	222	10
			layered	225	6
			layered	228	10
			layered	229	11
			layered	230	5
			layered	231	1

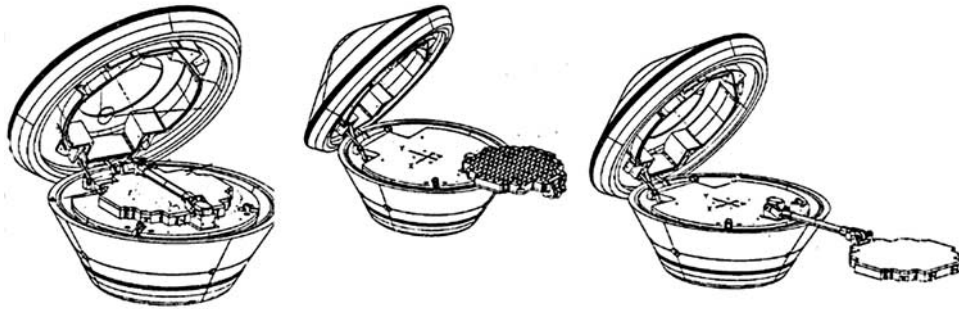


Figure 19. WISCER deployment sequence.

are inflight commanded with downlink telemetry to monitor hardware operation. This section describes these operational aspects pertinent to both Wild 2 and interstellar sample collections.

7.1. Sample Tray Assembly Operation

[112] The STA is tucked inside of the SRC. For sample collection, the STA has to be deployed by a controlled sequence of steps, similarly in the reverse sequence for the retraction.

7.1.1. Clamshell Opening

[113] The SRC was closed and locked at LMA after installation of the flight STA. To minimize exposure to outgassing contaminants, the SRC was held closed for 90 days in flight after launch to give the spacecraft time to outgas. The main heatshield clamshell latch was then released to allow outgassing of the SRC's internal components. The first full opening of the SRC was initiated at the first interstellar dust collection sequence on 16 February and retracted on 1 May 2000. At the end of the first interstellar collection period, the main heatshield clamshell was closed, but not latched. A similar deployment and retraction was carried out for the second interstellar collection sequence during the second orbit from 27 July through 9 December 2002. The main heatshield latch will not be activated until it is time for final closure of the clamshell after the Wild 2 encounter.

7.1.2. Sample Tray Assembly Deployment

[114] The initial STA deployment sequence was as follows: (1) Turn on the mechanisms and stepper motor heaters; (2) release the main heatshield clamshell latch; (3) open the clamshell (opening indicated by detent limit switches); (4) rotate the STA arm 180° from the base (position indicated by detent limit switches); and (5) rotate the STA from the end of the arm 180° (position indicated by detent limit switches).

[115] This deployment sequence is depicted in Figure 19. At the Wild 2 encounter, the STA will be fully extended and locked in a perpendicular position. The cometary collection surface faces the main dust shield and is orthogonal to the velocity vector of the approaching Wild 2 dust.

[116] In the stowed position, the interstellar tray faces up and the deployment arm is folded over it. The STA is deployed by two stepping motors mounted at the ends of the deployment arm. Deployment is accomplished in two steps (Figure 19). First the arm is rotated about its "elbow" point at the SC base plate from the stowed position. The STA is

then rotated about the "wrist" point to rise to its final position. A total of 960 motor steps are required for full extension. The heaters keep these motors within operating temperature range. Thermocouples on the motors monitor the motor temperatures. Since the STA is entirely passive, these two temperature readings, the number of steps of the motors makes, and the microswitches indicating motor stops at detent points provide the only real-time engineering telemetry from the WISCER.

7.2. Wild 2 Sample Collection

[117] It takes 5 years and about two and a third orbits about the Sun to bring the Stardust spacecraft to its rendezvous with comet Wild 2, all for 5 crucial min of sample collection. On 25 December 2003, 9 days before the closest encounter, the STA will be fully deployed poised for Wild 2 sample collection. Entrance into the outer portions of the Wild 2 coma will come about 5 hours before the closest approach. The majority of dust particles will be captured within a 5-min interval spanning closest approach. After exiting the Wild 2 coma, the STA will be retracted, the clamshell closed, and the latch activated. At that time, after the final set of limit switches has reached their detent positions, the SRC will be ready for Earth return.

7.3. Interstellar Sample Collection

[118] During the infall portions of the first two orbits, the STA was extended to collect interstellar particles on its back face. If the spacecraft was to maintain the collector pointing within $\pm 15^\circ$ of the interstellar stream for $\beta = 1$ particles during interstellar dust collection, the spacecraft would cast a shadow on the solar array some of the time. Thus, instead of adjusting the spacecraft attitude, the STA arm motor (in timed intervals) tilted to maintain interstellar stream tracking. However, during periods of Earth, communications performed at roughly biweekly intervals, the spacecraft must maneuver so that the high gain antenna points toward Earth on exposing the interstellar collector to β meteoroids.

[119] After the Wild 2 encounter, there is a third opportunity to collect interstellar dust particles during the infall portion of the last orbit. However, the high flux of Wild 2 dust particles could have damaged the aerogel capture cells and it was felt that a modest increase in the number of collected interstellar particles was not worth risking the primary Wild 2 samples. It was decided to forego the third interstellar dust collection; the main heatshield will be

closed, and the capsule lock activated, shortly after the cometary encounter. The next activation of the capsule lock will then be in the deintegration laboratory at JSC to begin the Preliminary Examination (PE) of the returned samples.

7.4. Earth Return

[120] After the Wild 2 and interstellar samples have been stowed, the spacecraft must cruise for approximately 2/3 of an orbital period before returning Earth. The spacecraft will target itself along a trajectory that just skims the Earth's upper atmosphere, cut the umbilical cord between the SCR and the spacecraft, and spin release the SRC on 15 January 2006. The spacecraft will then be diverted to miss the atmosphere and so continue its orbit about the Sun. The SRC entry angle has to be $-82^\circ \pm 0.08^\circ$ to ensure successful SRC reentry.

[121] It will take about 20 min from the Stardust spacecraft's release of the SRC to its landing in the Utah Test and Training Range (UTTR). Starting at an entry speed of 125 km/hr, a long sequence of events must be executed properly for a safe landing. These include ablative deceleration, release of the drone chute, release of the main chute, touchdown of the SRC in the flat regions of UTTR, and the ejection of the parachutes from the landed capsule to prevent wind dragging the SRC across the ground after landing.

[122] Stardust's Preliminary Examination Team (PET), UTTR Recovery Team, and LMA Operations Recovery Team, will race to recover the SRC. After locating the septum on the SRC, samples of gas will be taken from the within the SC and the PET prime execution phase will be initiated, as defined in the Preliminary Examination Plan (P. Tsou, unpublished data, 2002). The local contaminants in the touchdown area will be sampled. The SRC will be placed in a Class 10,000 shipping container with a dry N₂ environment for transportation to the processing site at JSC.

7.5. Preliminary Examination of the Samples

[123] Credible comprehensive findings from Wild 2 and interstellar samples will require decades of study by scientists in many laboratories around the world. However, a PE of the returned sample is part of the Stardust project plan. This is needed to provide a timely accounting of the mission as part of the NASA AO and is critical to provide a comprehensive assessment of the samples so it can be properly documented, curate and distributed for future scientific study. The PE will perform within the following constraints: (1) a 9-month period of analysis on Wild 2 samples and an additional year for the interstellar samples and (2) the number of samples to be analyzed is $\leq 25\%$ of the total returned samples.

[124] PE following SRC recovery includes deintegration of the Sample Subsystem, documentation of the returned samples and flight hardware, PE of selected samples, and report of PE findings. As part of the preparation for this PE period, methods to extract captured particles from aerogel unobtrusively need be developed and perfected [P. Tsou, unpublished data, 1992; Westphal et al., 2003].

7.6. Post Aerogel Delivery Characterization

[125] Although the WISCER is passive, calibration serves the critical purpose of establishing reference base-

lines in the aerogel from which to understand and interpret the returned samples. Chemical and physical reference baselines will be measured from at least one aerogel cell from each aerogel production run that was used for flight. Control cells were stored from each of the production batches for this purpose.

8. Conclusion

[126] WISCER accomplishes the core of the Stardust mission. The intact capture technology of hypervelocity particles and the development of methods and processes in working with silica aerogel are the critical innovations that enabled the Stardust sample return mission. These contributions added more tools for space exploration and enriching planetary science. It is anticipated that the analysis of the Wild 2 and interstellar samples returned by Stardust will contribute to a revolution of our understanding of comets, interstellar dust, and the raw materials from which our Solar System was made.

[127] **Acknowledgments.** This Stardust WISCER has been 20 years in the making. Direct and indirect assistance from scientists, managers, engineers, technicians, and benefactors who were touched by this dream and lent critical hands at critical moments made this possible. They came from the Ames Vertical Range, Brownlee's Laboratory at the University of Washington, the Chemistry and Material Science Laboratory of Lawrence Livermore National Laboratory, Lockheed Martin Astronautics, the Chemical Analysis Branch of the Los Alamos Laboratory, the Los Alamos Hypervelocity Microparticle Impacts Laboratory, the Physical Properties of Polymers and the Thermophysical and Mechanical Divisions and Solid Dynamics Department of the Sandia National Laboratory, the Max Plank Institut für Kernphysik, the Technische Universität München, the Ernst Mach Institut, the Physics Department of Oregon State University, the Geology and Biology Laboratory of Caltech, the McDonnell Center for Space Center at Washington University, the Experimental and Applied Mechanics Division of the University of Dayton, the Arnold Engineering Development Center, the Energy & Environment Division of the Lawrence Berkeley Laboratory, the Pruitt Research Center of Dow Chemical Company, the JPL Media Development Laboratory, and the Stardust Aerogel Team. Early guidance from A. Albee, J. Wasserburg, and H. Fechtig and valued assistance from J. Aubert, L. Hrubesh, P. Schultz, G. Tsou, J. Williams, and J. Weiss are especially recognized. J. W. Harris is specially recognized for his design of the sample collector and M. S. Hanner for her initial editing of this paper. This research was carried out at the Jet Propulsion Laboratory, California Institute of Technology, under a contract with the National Aeronautics and Space Administration.

References

- Anderson, W. W., and T. J. Ahrens, Physics of spacecraft-based interplanetary dust collection by impact into low-density media, *Tech. Rep. 94-05*, pp. 16–21, Lunar. and Planet. Inst., Houston, Tex., 1994.
- Anderson, J. D., E. L. Lau, M. K. Bird, B. C. Clark, G. Giampieri, and M. Pätzold, Dynamic science on the Stardust mission, *J. Geophys. Res.*, *108*(E12), 8117, doi:10.1029/2003JE002092, in press, 2003.
- Brownlee, D. E., The composition of cometary nuclei, in *Physics and Mechanics of Cometary Materials*, Rep. SEE N90-19989, pp. 12–90, Eur. Space Agency, Paris, 1989.
- Brownlee, D. E., et al., Stardust, NASA discovery proposal, *Internal Doc. D12181A*, Jet Propul. Lab., Pasadena, Calif., 1994.
- Brownlee, D., et al., Stardust: Comet and interstellar dust sample return mission, *J. Geophys. Res.*, *108*(E12), 8111, doi:10.1029/2003JE002087, in press, 2003.
- Burchell, M. J., R. Thomson, and H. Yano, Capture of hypervelocity particles in aerogel: In ground laboratory and low Earth orbit, *Planet. Space Sci.*, *47*, 189–204, 1999.
- Cinniger, A. G., Comet coma sample return—Hypervelocity intact capture experiments, *Internal Doc. D-3359*, Jet Propul. Lab., Pasadena, Calif., 1986.
- Deamer, D., J. P. Dworkin, S. A. Sandford, M. P. Bernstein, and L. J. Allamandola, The first cell membranes, *Astrobiology*, *2*, 371–381, 2002.
- Delsemme, A. H., The cometary connection with prebiotic chemistry, *Origin Life Evol. Biosphere*, *14*, 51–60, 1984.

- Engelbrecht, C., Analysis of gas collectors for comet coma sample return, *Interoff. Memo. 353PSA-86-208*, Jet Propul. Lab., Pasadena, Calif., 1986.
- Fujiwara, A., T. Mukai, J. Kawaguchi, and K. T. Uesugi, Sample return to NEA: Muses C, *Adv. Space Res.*, 25(2), 231–238, 1999.
- Griffiths, D. J., Comet coma sample return—Theoretical considerations of capture medium response for hypervelocity intact capture, *Internal Doc. D-6237*, Jet Propul. Lab., Pasadena, Calif., 1989.
- Grün, E., et al., Discovery of Jovian dust streams and interstellar grains by the Ulysses spacecraft, *Nature*, 362, 428–430, 1993.
- Grün, E., et al., Interstellar dust in the heliosphere, *Astron. Astrophys.*, 286, 915–924, 1994.
- Hanner, M. S., and T. L. Hayward, Infrared observations of comet 81P/Wild 2 in 1997, *Icarus*, 161(1), 164–173, 2003.
- Hohenberg, C. M., N. Thonnard, A. Berryhill, A. Glenn, K. Kehm, and A. Meshik, Status of volatiles collection option, paper presented at the Stardust Science Workshop, Stardust, Pasadena, Calif., 1996.
- Hörz, F., A small ballistic range for impact metamorphism studies, *Rep. TN D-5787/A-3181*, NASA Ames Res. Cent., Moffett Field, Calif., 1970.
- Hörz, F., M. J. Cintala, M. E. Zolensky, R. B. Bernhard, W. E. Davidson, G. Haynes, T. H. See, P. Tsou, and D. E. Brownlee, Capture of hypervelocity particles with low-density aerogel, *Rep. TM-98-201792*, NASA Johnson Space Cent., Houston, Tex., 1998.
- Hrubesh, L. W., Development of low density silica aerogel as a capture medium for hypervelocity particles, *Rep. UCRL-21234*, Lawrence Livermore Natl. Lab., Washington, D. C., 1989.
- Johannessen, C., Comet coma sample return—Intact capture track cavity study, *Internal Doc. D-5526*, Jet Propul. Lab., Pasadena, Calif., 1988.
- Keyvan, F., Hypervelocity intact capture—Projectiles and capture medium description, *Internal Doc. D-3467a*, Jet Propul. Lab., Pasadena, Calif., 1989.
- Kissel, J., et al., The cometary and interstellar dust analyzer for the Stardust mission, *J. Geophys. Res.*, 108(E12), 8114, doi:10.1029/2003JE002091, in press, 2003.
- Kromydas, W. M., Comet coma sample return—Hypervelocity intact capture data analysis, *Internal Doc. D-4678*, Jet Propul. Lab., Pasadena, Calif., 1987.
- Landgraf, M., and E. Grün, In situ measurements of interstellar dust, *Proc. IAU Colloq.*, 166, 381–384, 1998.
- Landgraf, M., M. Muller, and E. Grün, Prediction of the in-situ dust measurements of the Stardust mission to comet 81P/Wild 2, *Planet. Space Sci.*, 47, 1029–1050, 1999.
- Marsh, C. L., *Numerical Modeling of Detonations*, Univ. of Calif. Press, Berkeley, 1979.
- Martin, P. J., Launch profile pressure test, *Rep. P3574*, Jet Propul. Lab. Environ. Test Lab., Pasadena, Calif., 1998.
- McDonnell, J. A. M., et al., The dust distribution within the inner coma of comet P/Halley 1982i: Encounter by Giotto's impact detectors, *Astron. Astrophys.*, 187, 719–741, 1987.
- Mumma, M. J., Organic volatiles in comets: Their relation to interstellar ices and solar nebula material (abstract), *ASP Conf. Ser.*, 122, 369, 1997.
- Newburn, R. L., Jr., S. Bhaskaran, T. C. Duxbury, G. Fraschetti, T. Radey, and M. Schwochert, Stardust Imaging Camera, *J. Geophys. Res.*, 108(E12), 8116, doi:10.1029/2003JE002081, in press, 2003.
- Penland, R., Comet coma sample return—Intact captured projectile study, *Internal Doc. D-6672*, Jet Propul. Lab., Pasadena, Calif., 1989.
- Rogers, J., Aerogel and subscale aerogel containment development unit, *Stardust Flash Test Rep. SD-65300-500*, Lockheed Martin Astronaut., Littleton, Colo., 1996.
- Sandford, S., Filter test setup, *ARC Test Rep.*, NASA Ames Res. Cent., Moffett Field, Calif., 4 March 1997a.
- Sandford, S., Mold release comparison, *ARC Test Rep.*, NASA Ames Res. Cent., Moffett Field, Calif., 17 June 1997b.
- Sandford, S., Filter test results, *ARC Test Rep. 1-6*, NASA Ames Res. Cent., Moffett Field, Calif., 1998.
- Schulz, R., J. A. Stüwe, H. Boehnhardt, W. Gaessler, and G. P. Tozzi, Characterization of Stardust target comet 81P/Wild 2 from 1996 to 1998, *Astron. Astrophys.*, 398, 345–352, 2003.
- Sekanina, Z., A model for comet 81P/Wild 2, *J. Geophys. Res.*, 108(E12), 8112, doi:10.1029/2003JE002093, 2003.
- Snodgrass, L., Hypervelocity intact capture in Aerogel, *Internal Doc. D-7774*, Jet Propul. Lab., Pasadena, Calif., 1990.
- Tan, S., Trace metals analytical results, *Rep. WO 964278*, ChemTrace, Fremont, Calif., 1999.
- Tsou, P., Halley sample return experiment—Final report, *Internal Doc. D-797*, Jet Propul. Lab., Pasadena, Calif., 1983.
- Tsou, P., Intact capture of hypervelocity projectiles, *Int. J. Impact Eng.*, 10, 615–627, 1990.
- Tsou, P., Silica aerogel captures cosmic dust intact, *J. Non Cryst. Solids*, 186, 415–427, 1995.
- Tsou, P., Mir sample return experiment (MSRE), *Rep. 6-3, NASA Shuttle-Mir Phase 1 Res. Prog.*, NASA Johnson Space Cent., Houston, Tex., 1997.
- Tsou, P., and A. L. Albee, Effects of aerogel density on intact capture, *Proc. Lunar Planet. Sci. Conf.*, 23rd, 1453–1454, 1992.
- Tsou, P., and D. J. Griffiths, Exploratory investigation of hypervelocity intact capture spectroscopy, *Int. J. Impact Eng.*, 14, 751–761, 1993.
- Tsou, P., D. E. Brownlee, and A. L. Albee, Experiments on intact capture of hypervelocity particles, *Proc. Lunar Planet. Sci. Conf.*, 15th, Part 2, *J. Geophys. Res.*, 90, suppl., C866–C867, 1984.
- Tsou, P., D. E. Brownlee, and A. L. Albee, Intact capture of hypervelocity particles, *Tech. Rep. 86-05*, pp. 85–87, Lunar and Planet. Inst., Houston, Tex., 1986.
- Tsou, P., D. E. Brownlee, M. R. Lurance, L. Hrubesh, and A. L. Albee, Intact capture of hypervelocity micrometeoroid analogs, *Proc. Lunar Planet. Sci. Conf.*, 19th, 1205–1206, 1988.
- Tsou, P., J. Aubert, D. E. Brownlee, L. Hrubesh, J. Williams, and A. L. Albee, Effectiveness of intact capture media, *Proc. Lunar Planet. Sci. Conf.*, 20th, 1132–1133, 1989.
- Tsou, P., et al., Intact capture of cosmic dust analogs in aerogel, *Proc. Lunar Planet. Sci. Conf.*, 21st, 1264–1265, 1990.
- Tsou, P., D. E. Brownlee, J. M. Williams, and A. L. Albee, Effects of media mesostructure on intact capture, *Proc. Lunar Planet. Sci. Conf.*, 22nd, 1419–1420, 1991.
- Tsou, P., D. E. Brownlee, and A. L. Albee, Intact capture of hypervelocity particles on Shuttle, *Proc. Lunar Planet. Sci. Conf.*, 24th, 1443–1444, 1993.
- Tsou, P., R. H. Fleming, P. M. Lindley, A. Y. Craig, and D. Blake, Purity and cleanness of aerogel as a cosmic dust capture medium, *Proc. Lunar Planet. Sci. Conf.*, 25th, 1421–1422, 1994.
- Ward, P., T. Mottinger, P. Tsou, and K. Sherwood, Interface control document for Aerogel, *Rep. SD-622-210*, Lockheed Martin Astronaut., Littleton, Colo., 1997.
- Westphal, A. J., C. Snead, G. Domínguez, J. P. Bradley, M. E. Zolensky, G. Flynn, and D. Brownlee, An extraction and curation technique for particles captured in aerogel collectors, *Proc. Lunar Planet. Sci. Conf.*, 34th, 182–183, 2003.
- Zolensky, M., Filter test, *JSC Test Rep.*, NASA Johnson Space Cent., Houston, Tex., 21 April 1997.
- Zook, H. A., and R. W. High, Meteoroid capture cell construction, Patent 3971256, U.S. Patent and Trademark Off., Washington, D. C., 1976.

D. E. Brownlee, Astronomy Department, University of Washington, Box 351580, Seattle, WA 98195, USA. (brownlee@astro.washington.edu)

F. Hörz and M. E. Zolensky, NASA Johnson Space Center, MS SR, Houston, TX 77058, USA. (friedrich.p.horz@jsc.nasa.gov; michael.e.zolensky1@jsc.nasa.gov)

S. A. Sandford, NASA Ames Research Center, MS 245-6 Space Science Division, Astrophysics Branch, Moffett Field, CA 94035, USA. (sandford@mail.arc.nasa.gov)

P. Tsou, Jet Propulsion Laboratory, California Institute of Technology, Pasadena, CA 91109-8099, USA. (peter.tsou@jpl.nasa.gov)